ATMOSPHERIC ELECTRICITY

NEWSLETTER

Vol.34 No.2 2023 Nov

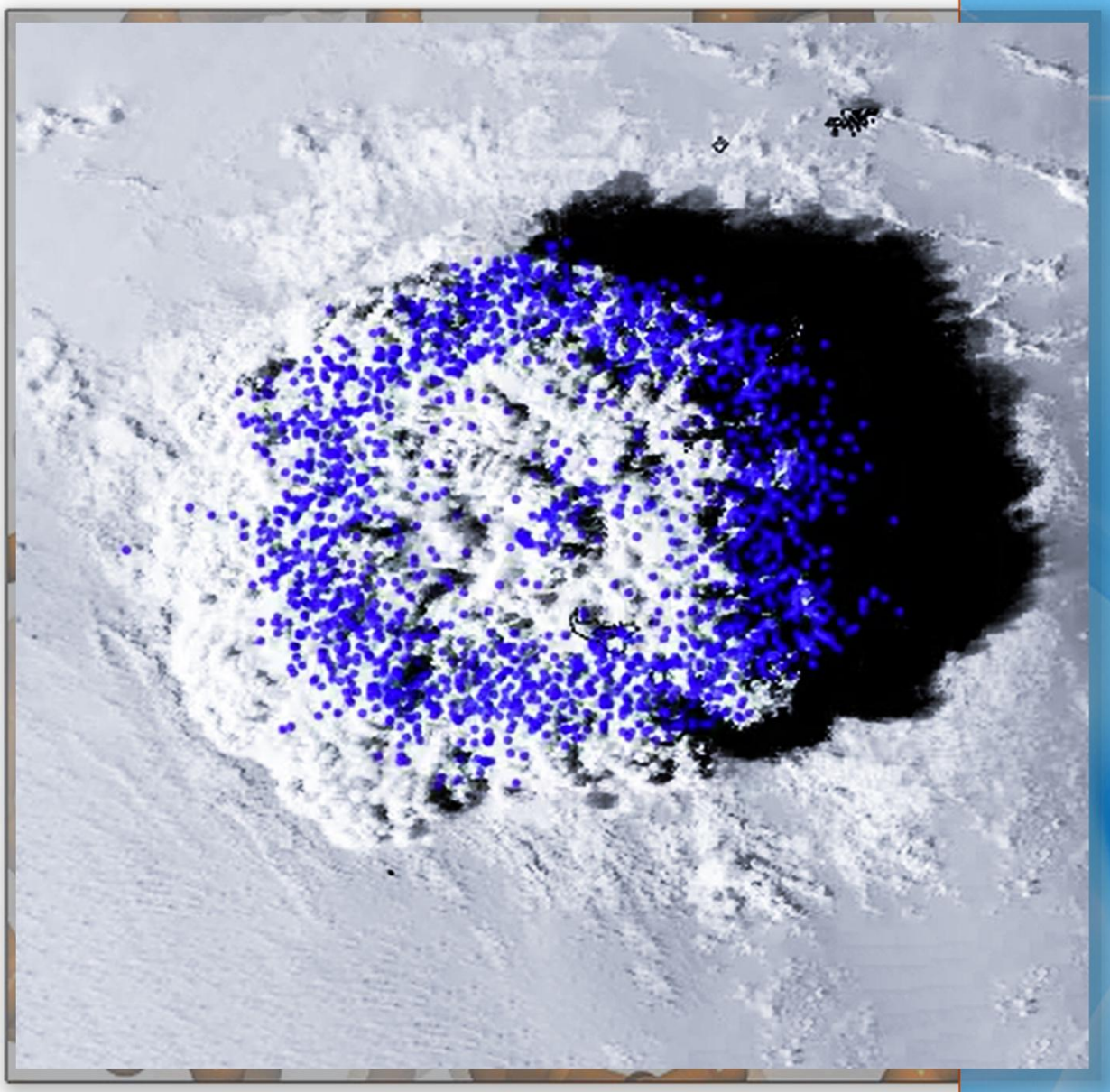

Cover Story :

The January 2022 eruption generated more than 192,000 lightning flashes and sent a volcanic plume of ash 58 kilometers into the sky. Several concentric rings were observed that seemed to be linked to each explosive outburst from the volcano.

More details are found in the paper by Van Eaton A. R., et al. 2023, *GRL*, e2022GL102341. https://doi.org/10.1029/2022GL102341

ICAE

IAMAS IUGG

https://www.iamas.org/icae/

2024 EGU

37th International Conference on Lightning Protection

The ICLP 2024 will be held in the city of Dresden, Germany. Please submit a paper no later than February 1st, 2024 at https://www.iclp2024.org/en.

New AGU Fellow

Dr. Xiushu Qie, from the Institute of Atmospheric Physics, Chinese Academy of Sciences, was awarded the 2023 AGU Fellowship for breakthrough contributions to our understanding of storms over Tibetan Plateau and fundamental properties of natural and triggered lightning. (https://www.agu.org/honors/announcement/union-fellows)

Congratulations!

ALOFT Field Campaign Searches for Gamma-Rays Above Tropical Thunderstorms

Timothy Lang and Nikolai Østgaard

The ALOFT* airborne campaign occurred during 1-30 July 2023. The campaign used the NASA ER-2 to overfly tropical thunderstorms in the Americas to hunt for lightning and gamma-ray emissions. ALOFT was a tremendous success, detecting many terrestrial gamma-ray flashes (TGFs), as well as many gamma-ray glows. ALOFT also gathered dozens of hours of validation data for spaceborne lightning detectors like the International Space Station Lightning Imaging Sensor (ISS LIS) and the Geostationary Lightning Mappers (GLMs), and tested new concepts for future lightning detection from space. Finally, ALOFT made observations of convection relevant to upcoming NASA missions like the Atmosphere Observing System (AOS). The ER-2 payload featured two gamma-ray sensors, multiple lightning and electric field sensors, two microwave radiometers, and X-band and W-band radars. ALOFT also featured numerous ground-based lightning and high-energy sensors stationed throughout the Americas, which were often the focus of the ER-2 flights. These sensors included two- and three-dimensional VHF lightning mappers and interferometers, as well as a regional network of LF antennas. Several other ground sensors were involved as well. The ALOFT mission is a partnership between NASA, the University of Bergen (UIB), and several other institutions. The principal investigator for ALOFT is Nikolai Østgaard (UIB). The NASA project scientist is Timothy Lang. ALOFT data are expected to be made public through NASA Earthdata (https://www.earthdata.nasa.gov/) in early 2024. The ALOFT website may be found at https://www.uib.no/en/aloft. A video highlighting airborne operations during ALOFT can be found at https://www.youtube.com/watch?v=qFEtaGJ-ZAs.

*ALOFT = Airborne Lightning Observatory for FEGS and TGFs

FEGS = Fly's Eye GLM Simulator

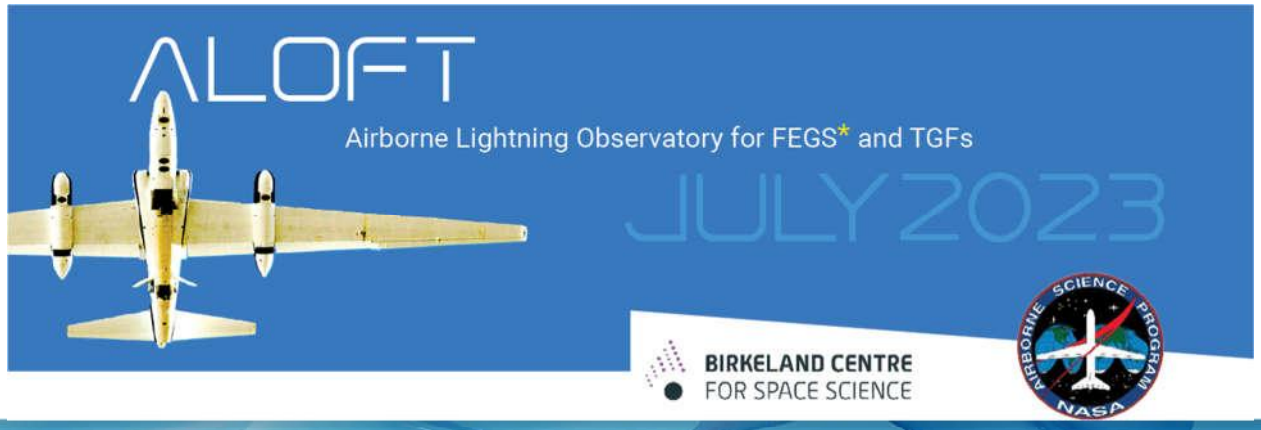

International Space Station Lightning Imaging Sensor Decommissioned

Timothy Lang

On Thursday, 16 November 2023, at approximately 2117 UTC, the International Space Station Lightning Imaging Sensor (ISS LIS) was powered off and decommissioned. This was a planned event to make way for the Atmospheric Waves Experiment (AWE), which will take over the location that ISS LIS was occupying. The decommissioning was coordinated with the Space Test Program (STP), which managed the host payload that contained ISS LIS along with several other experiments. ISS LIS had operated on orbit for nearly 6.75 years, with operations starting back in March 2017. The mission extended the global record of lightning observations from space, both in time (this record originally started back in 1995 with the Optical Transient Detector, OTD) and in latitude (by broadening observations to +/-55° relative to the LIS instrument on the Tropical Rainfall Measuring Mission, TRMM, which only viewed to +/38°). ISS LIS also provided near-realtime (NRT) lightning observations to operational end users, such as the US National Weather Service (NWS). In recent years ISS LIS observed a significant reduction on tropical lightning, possibly due to the COVID-19 pandemic and an especially strong La Niña climate pattern around 2020-2021. This was an unprecedented event in the nearly 30-year record of lightning from OTD and TRMM/ISS LIS. During the next two years, the LIS team will harmonize and combine the full OTD + TRMM/ISS LIS datasets, creating a climate data record for global lightning from space. The mission scientist for ISS LIS is Timothy Lang (NASA Marshall), who succeeded the original principal investigator (PI), Rich Blakeslee, in 2020. ISS LIS operated well up until the decommissioning, with the final orbit (Figure 1) capturing nearly 300 lightning flashes.

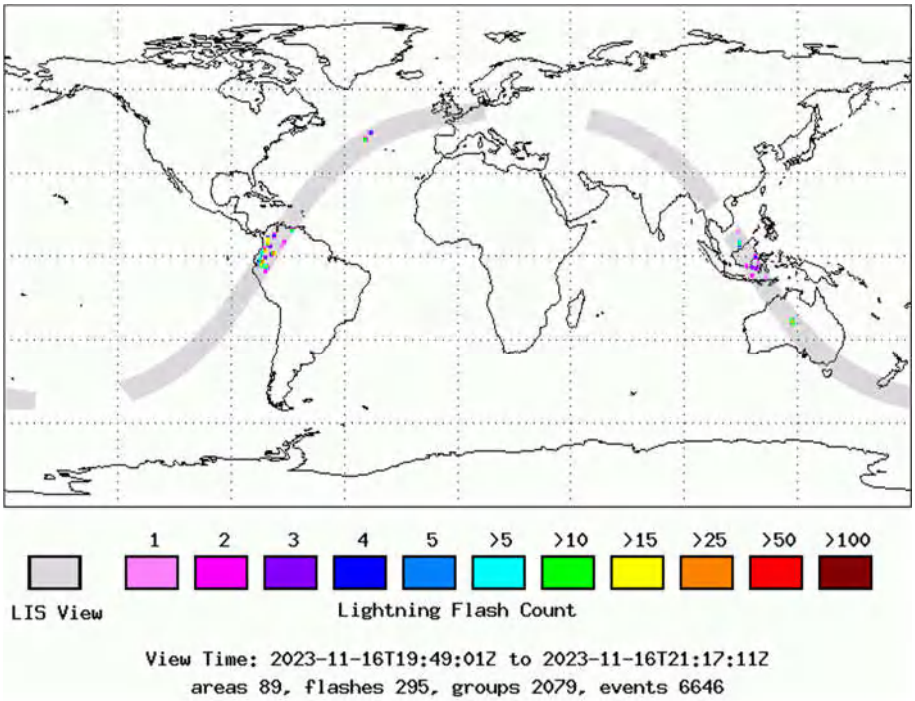

Figure 1. Quicklook NRT image of showing the lightning observed within the ISS LIS swath during its last orbit. The occasional swath gaps are caused by NRT communication outages.

Stanisław Michnowski (1918-2023)

Stanisław Michnowski during the celebration of his 100th birthday at the Institute of Geophysics on November 13th, 2018. Photo credits: Anna Zdunek, Institute of Geophysics PAS, Warsaw.

A pioneer of modern atmospheric electricity research in Poland, Stanisław Michnowski, passed away in Warsaw on July 28, 2023 at the age of 104. He was born on November 10, 1918, in Mlodzawy, Poland, now part of Skarzysko-Kamienna. In 1937 he became a student at the Faculty of Electrical Engineering of Warsaw Polytechnic. The outbreak of Second World War interrupted the studies. In the battles of September 1939 he took part as a volunteer, and later was engaged in underground activity. Eventually he become a soldier of the Home Army and its Directorate of Diversion, after he managed to avoid arrests and the massacres of the people in Skarzysko in 1940. After the war he resumed studying at the Warsaw Polytechnic and also enrolled at the Faculty of Physics at the University of Warsaw. In the senior university years he worked as a research assistant. After the graduation he was not allowed a job position at the Polytechnic because of political reasons. Permanent employment was granted to him in 1954 by the Department (now Institute) of Geophysics, Polish Academy of Sciences, where he became the Head of the Laboratory of Atmospheric Electricity in the Department of Atmospheric Physics. Michnowski started his job with organizing a modern atmospheric electricity station at the Magnetic Observatory in Swider near Warsaw, where he previously performed some atmospheric electricity research related to corona discharges. In 1957 he joined the projects of the International Geophysical Year, taking part in the Polish Expedition to North Vietnam. There he led the work to establish the atmospheric electric station at Sa-Pa and Phu-Lien, gave lectures, led seminars, and wrote a handbook on atmospheric electricity published in Vietnam in 1960. After the return to Poland, followed by a 1-year fellowship in Great Britain, his research work concentrated on the interpretation of the variations of the electric field produced by lightning discharges in inhomogeneous media such as the Earth's atmosphere - one of his greater achievements in thunderstorm electricity science which

gave him recognition in the international atmospheric electricity community. Another of his achievements was an innovative analysis of the location and sequence of lightning strokes to assess the electrical structure of a Mesoscale Convective System, published in 1987, a project undertaken jointly with the University of Uppsala, Sweden, and Polish Institute of Meteorology and Water Management. He obtained a doctoral degree in 1972 and in 1984 he became a docent. In later years he continued thunderstorm research mentoring his students from Poland and from Vietnam. He headed the Atmospheric Electricity Laboratory until his retirement. There he created a successful collaborative scientific environment with multiple contacts in other Polish institutions and universities, and visits of colleagues and students from abroad. In the late 1980s the expansion of the Institute's research at the Polish Polar Station in Hornsund, Spitsbergen, opened a new chapter in the projects of the group. The research, supported by the new collaborators from the Institute of Physics of the Earth, Russian Academy of Sciences, was aimed at investigating the effects of the coupled solar wind, magnetosphere and the ionosphere on the electricity of the lower atmosphere, using data from Hornsund and Swider. A review of the results of these studies has been the subject of the activities of Stanislaw Michnowski during his retirement and was published in 2021. This was the last position in the list of over 120 his own and co-authored publications on atmospheric electricity.

He was an inspiring and enthusiastic, albeit demanding supervisor and mentor. He was always a great organizer. He reached out to people, always trying to involve them in a collaborative work, and liked to organise seminars and informal meetings. In the Polish Geophysical Society Michnowski was the founding member of the Society's Department of Physics of the Earth's Interior and Near-Earth Space. He actively supported the activities of the organization until the end, having been an honorary chairman of the branch. Michnowski's activity and merits have been acknowledged by Polish and international scientific community. He was an Honorary Member of Polish Committee on Lightning Protection, and Honorary Member of Polish Geophysical Society. In November 2014 he was elected an Honorary Member of the International Commission on Atmospheric Electricity, after four decades of serving as a member of the Commission. In 2018 he celebrated the grand jubilee of hundred years of age. He is survived by two daughters Anna and Maria, and his grandson Karol, and is missed dearly by family, friends and colleagues.

More information about the life of Stanisław Michnowski can be found in the commemorative publication in Publs. Inst. Geophys. Pol. Acad. Sc., 424 (D-74), doi: 10.25171/InstGeoph_PAS_Publs-2018-085, and in Przeglad Geofizyczny 64 (1-2), 185-194, doi: 10.32045/PG-2019-006.

Atmospheric Electricity Group at the Institute of Geophysics PAS

Stanislaw Michnowski (1918-2023): Maverick of the Global Electrical Circuit

Stanislaw Michnowski long-championed the measurement of the Earth's global electrical circuit (GEC) in a research career whose length has now eclipsed that of C.T.R. Wilson, and which continued through his 100th birthday celebration in Warsaw (in which I was fortunate to participate with other Polish colleagues in atmospheric electricity: Piotr Baranski, Marek Kubicki, Mariusz Neska and Anna Odzimek). Living more than four additional years until July 28, 2023, Stanislaw now holds the world record as the oldest atmospheric electrician. (The earlier record holder, Hans Dolezalek, died in 2015 at age 103.)

Stanislaw's utilization of three measurement sites for atmospheric electricity at different latitudes: Swider in Poland (52N) in the late 1950s, Cha-Pa in Vietnam (22N) in the 1960s, and Hornsund in Spitsbergen (77N) in more recent decades, has enabled a broad perspective on the behavior of atmospheric electrical variables.

With his knowledge that tropical convection dominated the source of the GEC, Stanislaw established an observatory far from home at Cha-Pa in North Vietnam. With his knowledge that point discharge dominated the "balance sheet" for charge transfer to Earth, one of his first research publications explored this topic in detail.

While in Vietnam, a country adjacent to the sea, Stanislaw had access to a large population of 'warm' clouds. As a young researcher at the time, he had the audacity to publish an observation revealing two lightning flashes in a cloud he documented to be in the 'warm' category. This finding, throwing a wrench into ice-based theories for cloud electrification and also the idea that the polarity of the GEC was dictated by some special property of ice, also fired the enthusiasm of advocates of the convective theory for storm electrification (Bernard Vonnegut and Charles Moore) at the time.

Throughout his career Stanislaw kept an eye on the behavior of the "fair-weather" electric field, both at Swider and at Cha-Pa. Based on monitoring at Swider, he came to realize the challenges to globally representative signals against the local noise of the polluted continental boundary layer. Undeterred by this disquieting news, he changed his focus and main observational attention to higher latitude (Hornsund) where the air pollution was much reduced (but where wind effects and magnetospheric/solar wind disturbances were unfortunately problematic). Today, the Hornsund station includes a Schumann resonance receiver, serving as key verification for the global representativeness of the AC global circuit from a single measurement site.

Earle Williams

African Centres for Lightning and Electromagnetics Network (ACLENet)

ACLENet continues to address the huge gap in understanding and preparedness from the lightning threat in Africa compared with many other parts of the world. While the effort is small and the need is large, prototype ACLENet activities can spread through constant reminders and efforts to lightning interests such as readers of the ICAE Newsletter.

These issues were apparent when lightning caused a fire at a girls' school in Uganda that destroyed an on-campus dormitory. Fortunately, no one was in the building at the time since classes had started. The school may have had inadequate lightning protection. See https://www.youtube.com/watch?v=uT1SEqm6yiE and https://www.monitor.co.ug/uganda/news/national/property-destroyed-as-fire-burns-st-theresa-kisubi-girls-dormitory-4412926.

This year, a national advisory board has been established in Uganda. This advocacy group has begun to be trained so that they can be a resource for the increasing number of queries from in-country as lightning is gradually recognized as a significant and manageable natural hazard.

ACLENet continues to maintain the only and largest database of lightning deaths, injuries, and damages in the world at https://aclenet.org/news-publications/country-news/directory-of-countries.html.

In addition, the ACLENet Newsletter is now translated into French, Portuguese, Spanish, and Arabic and can be viewed at https://aclenet.org/news-publications/newsletters/mailing-list.html.

Additional support for ACLENet activities is evidenced by the following connections:

- An Asian company is ready to provide materials for a lightning protection system at another school in Uganda – our eighth.
- A USA company is working with us to protect a ninth school.
- A large tea farm operator in Rwanda has asked ACLENet to review protection and safety policies for lightning.
- A European company with possible external funding has approached ACLENet about providing lightning warnings at schools in Uganda with lightning protection systems.

Readers of this Newsletter are encouraged to consider ways that they can support this wide-ranging activity in Africa through donations or in-kind support. See https://ACLENet.org and choose 'Contact Us'.

Department of Physics, Loyola University of Chicago

Rasha Abbasi

First high-speed video camera observations of a lightning flash associated with a downward terrestrial gamma-ray flash. Terrestrial Gamma-ray Flashes (TGFs) are bursts of high energy photons of sub millisecond duration that are produced by lightning. The study of TGFs, both their initiation and propagation, is of major interest to lightning researchers. While it is known that TGFs are produced inside thunderstorms and in correlation with lightning, mechanisms responsible for producing TGFs and the relation of intra-cloud discharges to TGFs are still unknown.

In September of 2021, The Telescope Array Surface Detector (TASD), a 700 km^2 cosmic ray detector located in the western desert of Utah, U.S.A. observed an energetic downward-directed terrestrial gamma-ray-rate-producing thunderstorm. This storm was responsible for a significant fraction of all ground TGFs detected over the TASD in the past ten years.

In a recent publication (Abbasi, R. U., Saba, M. M. F., Belz, J. W., Krehbiel, P. R., Rison, W., Kieu, N., et al. (2023). First high-speed video camera observations of a lightning flash associated with a downward terrestrial gamma-ray flash. *Geophysical Research Letters*, 50, e2023GL102958. doi:10.1029/2023GL102958), we discussed the first simultaneous detection of one of those downward-directed TGFs using a high-speed video camera, the Telescope Array detector, in addition to a suit of lightning instruments. This allowed us to understand in detail the height, speed, optical luminosity, footprint, energy deposit, and stage of lightning in the flash that is associated with gamma-ray bursts observed by the TASD detector. The advantage of proximity to the source and the use of a suite of lightning instruments together with the high-speed camera made possible further understanding of the characteristics of lightning processes associated with TGF production. It also allowed us to compare the optical emission observations of lightning discharges associated with downward vs. upward-moving TGFs (Figure 1).

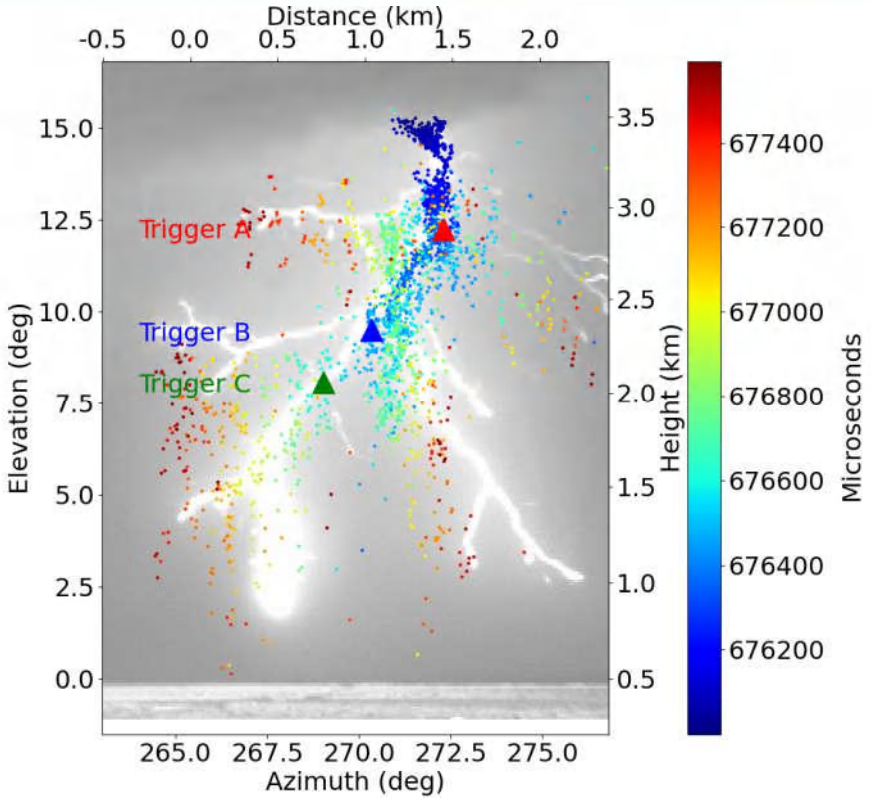

Figure 1. Plot shows the elevation vs. azimuth for a flash using 40,000 fps high-speed video camera in addition to Interferometer point sources. The filled triangles indicate to the source height for each gamma-ray trigger. More details are found in the paper Abbasi et al. (2023).

Department of Space Physics, Institute of Atmospheric Physics of the Czech Academy of Sciences

Ivana Kolmasova

The collaboration between the Institute of Atmospheric Physics of the Czech Academy of Sciences and the atmospheric electricity group from Laboratoire d'Aerologie CNRS in Toulouse, France, led by Eric Defer, has focused on analyzing data obtained from the broadband magnetic loop antennas SLAVIA (Shielded Loop Antenna with a Versatile Integrated Amplifier) and the Lightning Mapping Array SAETTA (Suivi de l'Activité Electrique Tridimensionnelle Totale de l'Atmosphère) since 2015. During this period, the IME-HF analyzer (Instrument de Mesure du champ Electrique Haute Fréquence) prototype, initially developed for the TARANIS (Tool for the Analysis of Radiation from lightning and Sprites) mission, was adapted for ground-based measurements. It was coupled with the SLAVIA antenna and installed in the northernmost part of Corsica. The analyzer already survived several damages

caused by bad weather and the strong Mediterranean winds stole the original makeup of the antenna (Figure 1). The dedicated efforts of our resilient engineer, Radek Lán, and the collaborative support from our colleague Dominique Lambert in Toulouse have played a crucial role in keeping the system operational.

Thus far, we have collaboratively published three papers, which gained from the complementary information acquired by both antenna types. The broadband magnetic field recordings sampled at 80 MHz provide valuable insights in the evolution stage of investigated lightning discharges and SAETTA identifies and localizes the radiation sources. We investigated in detail the initial breakdown phase of negative cloud-to-ground (CG) lightning discharges [1] and inverted intracloud flashes [2]. In both these papers, we for the first time used the raw LMA data. This approach revealed a nearly continuous Very High Frequency (VHF) radiation presence during the initiation phase of lightning discharges. Consequently, different LMA stations detected various peaks, occasionally challenging the processing algorithm to align them accurately. As a result, surprisingly small amount of sources was localized during the initiation phase. In our third paper [3], we extended our investigations to the processes occurring immediately after the first return strokes in both positive (Figure 2) and negative CG discharges. We also cooperate with Earth Networks to identify Narrow Bipolar Events in our broadband data.

[1] Kolmašová, I., Santolík, O., Defer, E., Rison, W., Coquillat, S., Pedeboy, S., et al. 2018. Lightning initiation: Strong VHF radiation sources accompanying preliminary breakdown pulses during lightning initiation. Scientific Reports, 8(1), 3650. doi:10.1038/s41598-018-21972-z.

[2] Kolmašová, I., Santolík, O., Defer, E., Kašpar, P., Kolínská, A., Pedeboy, S., Coquillat, S. 2020. Two propagation scenarios of isolated breakdown lightning processes in failed negative cloud-to-ground flashes. Geophysical Research Letters, 47, e2020GL090593. doi:10.1029/2020GL090593.

[3] Kolínská, A., Kolmašová I., Santolíl, O., Defer. E. and Pedeboy. S. 2022. Electromagnetic radiation of cloud-to-ground lightning flashes detected by broadband receiver BLESKA and narrowband SAETTA stations, WDS'22 Proceedings of Contributed Papers — Physics, 65–69, 2022. 978-80-7378-477-5 © MATFYZPRESS.

Figure 1. Broadband shielded magnetic loop with an integrated preamplifier installed at Cap Corse, Corsica, France.

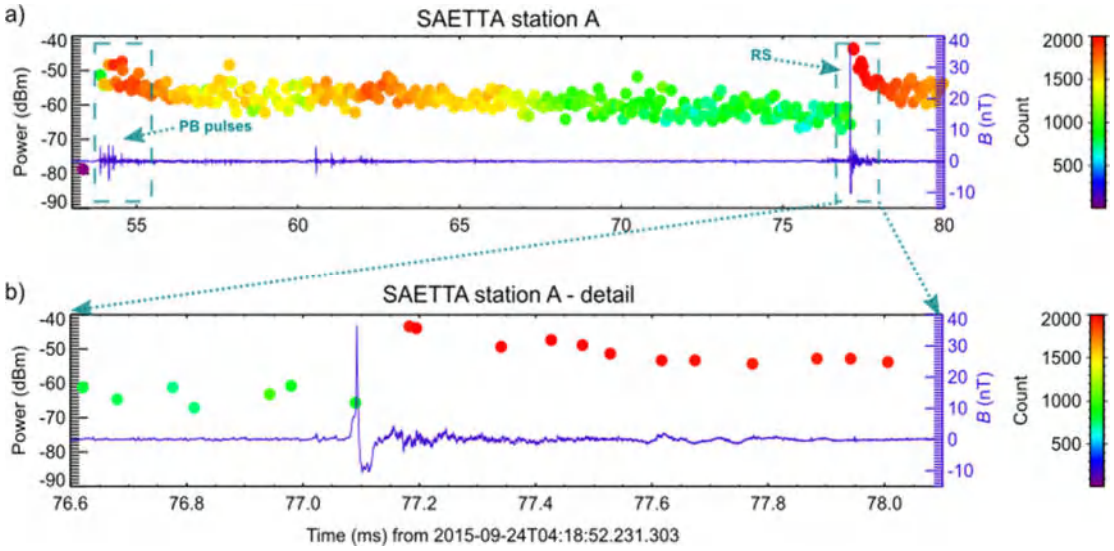

Figure 2. An example of a +CG flash starting on 24th September 2015 at 04:18:52.231303 UT: a) the broadband record (blue waveform) with peaks of radiated VHF power recorded at SAETTA station A (color coded by their count in individual 80 μs LMA time intervals); b) a detail of the RS peak.

HUN-REN Institute of Earth Physics and Space Science, Sopron, Hungary

Contributors: *József Bór, Tamás Bozóki, Attila Buzás, Ernő Prácser, Gabriella Sátori, Karolina Szabóné André, José Tacza*

Professor Earle Williams (MIT, USA) is spending the last 3 months of 2023 with the Atmospheric Physics research unit of the HUN-REN Institute of Earth Physics and Space Science as a distinguished visiting scientist in the framework of the corresponding programme of the Hungarian Academy of Sciences. The cooperation of the research unit with Professor Williams has been active for three decades now and resulted in several visits and numerous joint publications already. The current visit serves to make progress in research topics which cover relevant open questions in atmospheric sciences regarding the utilization of atmospheric electricity measurements, and specifically that of Schumann resonances (SRs), as tools for monitoring the variations of the global lightning activity. During the visit, the possibilities of making globally representative measurements of the Wilson current in the atmosphere are explored by utilizing long transmission lines (at least several hundreds of meters long) which are out of regular use as power lines or telephone lines.

In the paper by Bozóki et al. (2023) day-to-day variations of global lightning activity has been investigated based on SR intensity records from 18 SR stations around the globe and independent lightning observations provided by ground-based (WWLLN, GLD360, and ENTLN) and satellite-based (GLM, LIS/OTD) global lightning detection. We showed that by summing the intensity of the first three SR modes of the two magnetic field components and by averaging these values on a daily basis, a quasi-global invariant quantity can be obtained that can serve as a very valuable tool to investigate day-to-day changes in global lightning activity. This quantity revealed significant variability (a factor of 2–3 on the time scale of 3–5 days) in the overall intensity of global lightning activity that can occur within a few days and is likely explained by continental-scale temperature changes related to cold air outbreaks from polar regions. Independent global lightning data sets (especially Earth Networks Thunder Hours) showed good agreement with the variations of the quasi-global invariant quantity (Figure 1). Furthermore, our study clearly demonstrated that detailed investigation of lightning on global/continental scales is currently hindered by the incomplete and spatially uneven detection efficiency of ground-based global lightning detection networks and the restricted spatio-temporal coverage of satellite observations

which underlines the need for improving the available observation methods and calculation techniques in this respect.

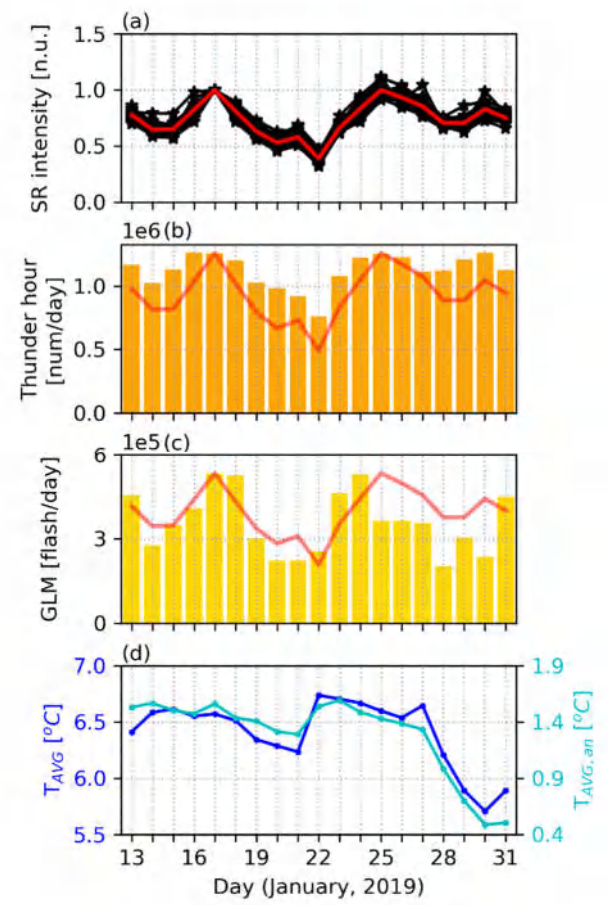

Figure 1. Comparison of (a) normalized daily average SR intensity records (in normalized units) with (b) total daily numbers of Earth Networks Thunder Hours, (c) daily flash rates provided by GLM and (d) daily global mean land surface temperatures (T_{AVG}, NOAA CPC) and temperature anomalies ($T_{AVG,an}$, Berkeley Earth). GLM-detected lightning flashes had been summed on a daily basis for South America. In the top subplot black curves correspond to different SR stations while the red curve shows the average of all records. The scaled version of the latter curve is also displayed on subplots (b) and (c).

In connection with the visit of Professor Earle Williams, we collected data from more than 25 ELF/SR stations around the globe for the January 2022 major eruption of the Hunga-Tonga volcano (Figure 2). The exceptional amount of lightning activity produced by this event (lightning in the eruption dominated the naturally occurring global lightning activity for a period of at least 1 hour) provided a highly localized source of excitation for the SRs, and so represents a unique opportunity to test SR models, which usually assume a point source of excitation (see Bór et al., 2023 for more details about the eruption). If readers of this Newsletter

are aware of any ELF/SR stations that were in operation on 15 January 2022 and do not appear on our map, please contact us. A preliminary result of this investigation is that by removing transient signals (Q-bursts) generated by powerful lightning discharges, we obtain "whiter" SR spectra, which are in remarkably better agreement with the modeled spectra (assuming dirac-delta excitation). This is in line with Ogawa's original description of Q-bursts as having higher energy around the fundamental SR mode (red spectrum). An important question for us at the moment is how to define the amplitude limit above which the transients are removed.

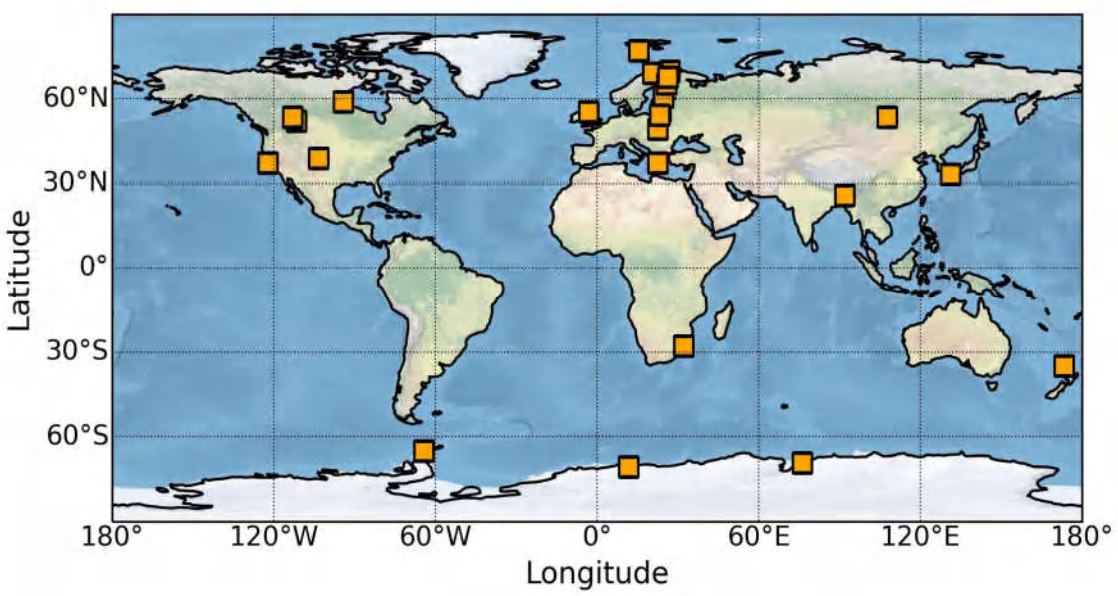

Figure 2. Map of ELF/SR stations used to study Schumann resonances in relation to the major eruption of the Hunga-Tonga volcano on 15 January 2022.

A surprising discovery was made in the frequency variations of the 3rd Ez mode between two nearby SR observation sites (NCK, Hungary and AGO, Slovakia) with about 90 km distance difference from each other. One could expect very high similarity between the diurnal frequency patterns in such a short distance (as compared to the wavelength of SRs). Instead, opposite frequency variations can be observed in early morning and late evening UT hours in winter months. The SR model computations developed by Ernő Prácser seem to have a plausible explanation for this observation using simulations with extended lightning sources.

Recently, it has been shown that there are changes in the length of seasons based on temperature measurements. In the Northern Hemisphere, summers have become longer while winters have become shorter. Building on this finding, we are now investigating whether there are corresponding changes in the length of seasons based on global lightning activity, which

we refer to as "electromagnetic seasons". To conduct this study, we are using SR measurements, which serves as a proxy for global lightning activity. We are analyzing the diurnal variation of SR daily peak frequencies for the first and second mode. The data we are using covers the period from 1994 to 2016 and was collected at the Nagycenk Geophysical Observatory using a ball antenna that recorded the vertical electric field component. Preliminary results indicate an increase in the duration of summer electromagnetic seasons in both hemispheres. These findings were presented at the IUGG 2023 conference, and we are currently preparing a manuscript on this topic.

Institute of Atmospheric Physics, Chinese Academy of Sciences (IAP, CAS), Beijing, China

Characteristics of negative breakdowns in extinguished channels of a positive cloud-to-ground flash. The characteristics of a natural positive cloud-to-ground lightning flash which had only one return stroke are investigated in detail using synchronous detections of lightning very-high-frequency (VHF) interferometer, fast antenna, high-speed video and S-band Doppler weather radar. The flash initiated at 5.8 km above the ground and at the edge of an enhancing convective cell, where a positive bi-level charge structure was involved. The initial negative leader developed upward, forming multiple branches, while the positive leader was recognized 22.2 ms later. The breakdown with different polarities exhibited distinct properties. Three significant negative breakdowns initiating in the previously established but extinguished negative channels were well detected by the VHF interferometer, with a duration of 0.30 ms, 0.06 ms and 0.20 ms, and propagation speed of 1.9×10^6 m/s, 2.2×10^7 m/s and 1.9×10^7 m/s, respectively. The first one occurred 0.3 ms before the return stroke, its occurrence promoted the development of the downward positive leader that was getting close to the ground, leading to an obvious acceleration and an enhancement of the channel luminosity. The second and the third negative breakdowns occurred during the continuing current after the return stroke, acting as the causation of the positive M-components. Symmetric V-shaped and hooked pulses on the fast electric field change waveform and obvious increased luminosity of the grounded channel were well detected. The occurrence of negative breakdowns in the pre-conditioned channels served for producing a backward surged current wave that promote the discharge process through the grounding/grounded channel. (Tang

G. et al., 2023, AR)

A parallax shift effect correction based on cloud top height (CTH) for FY-4A Lightning Mapping Imager (LMI). We proposed an ellipsoid CTH parallax correction (ECPC) model for lightning positioning applicable to FY-4A LMI. The model utilizes CTH data from the Advanced Geosynchronous Radiation Imager (AGRI) on FY-4A to correct the lightning positioning data. According to the model, when the CTH is 12 km, the maximum deviation in lightning positioning caused by CTH in Beijing is approximately 0.1177° in the east–west direction and 0.0530° in the north–south direction, corresponding to a horizontal deviation of 13.1558 km, which exceeds the size of a single ground detection unit of the geostationary satellite lightning imager. Therefore, it is necessary to be corrected. A comparison with data from the Beijing Broadband Lightning Network (BLNET) and radar data shows that the corrected LMI data exhibit spatial distribution that is closer to the simultaneous BLNET lightning positioning data. The coordinate differences between the two datasets are significantly reduced, indicating higher consistency with radar data. The correction algorithm decreases the LMI lightning location deviation caused by CTH, thereby improving the accuracy and reliability of satellite lightning positioning data. The proposed ECPC model can be used for the real-time correction of lightning data when CTH is obtained at the same time, and it can be also used for the post-correction of space-based lightning detection with other cloud top height data (Figure 1, Zhang Y. et al., 2023, Remote Sens.).

Estimation on lightning activity of squall line by new lightning parameterization schemes in WRF model. Based on three-dimensional lightning data and S-band Doppler radar, a strong relationship was identified between lightning activity and the volume of radar echo. A detailed analysis of the squall line investigated the relationship followed an exponential function. According to the correlation between lightning and the radar volume, new lightning parameterization schemes, named as the V30 dBZ, V35 dBZ and V40 dBZ lightning schemes, has been established and introduced into the weather research and forecasting (WRF) model. The simulation of typical squall lines was conducted, and found that the simulated the dynamics and microphysics basically reproduced the observed convective structure. the performance of different lightning parameterization schemes, including the new radar-volume-based schemes (V30 dBZ, V35 dBZ, and V40 dBZ), as well as existing schemes (PR92_1, PR92_2, and LPI-Lightning Potential Index), was evaluated. The evaluation showed that the simulated lightning activity using the radar volume-based schemes was more consistent with the observations (Figure 2), although there were some differences in the spatial and temporal distribution of lightning activity among different lightning schemes. The radar-volume-based lightning

parameterization schemes, proved to be reliable in estimating lightning activity when compared to the observations (Liu et al., 2023, Remote Sens.).

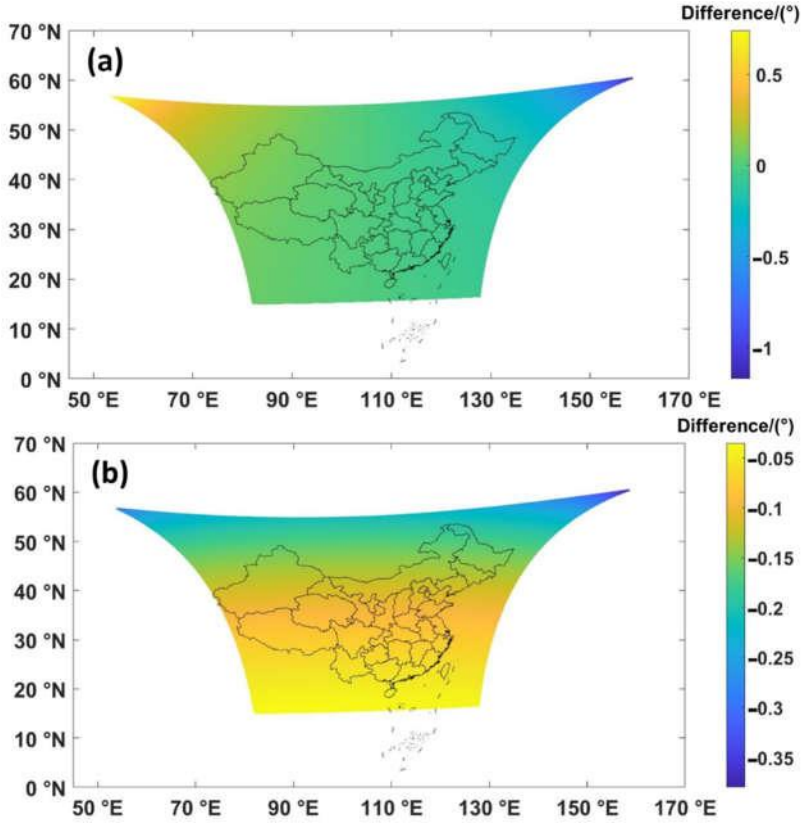

Figure 1. ECPC model simulation correction results. (a) Longitudinal deviation in lightning positioning under 12 km CTH (negative values indicate westward correction; positive values indicate eastward correction), (b) Latitudinal deviation in lightning positioning under 12 km CTH (negative values indicate south-ward correction).

Detailed modeling and evaluation of the potential impact of blue jet on the atmospheric chemistry. Blue jet (BJ) is a type of upper atmospheric discharge which produces nitrogen oxides (NO_x=NO+NO_2) through the same chemical reactions as the tropospheric discharges. As stratospheric NO_x contributes to ozone depletion and BJ occurs at the altitude of the stratospheric ozone layer, this study estimates its chemical effects in the stratosphere using a detailed plasma-chemistry model, focusing on the chemical families of oxygen, nitrogen, chlorine, and bromine. The results obtained during the first 100 s indicate the ozone enhanced in the middle stratosphere, while no obvious change in the lower and close to the top of the stratosphere. After two days, simulations show that the entire neutral chemical stratospheric system is modified with the enhancement of nitrogen oxides, chlorine, and bromine reservoirs. As a consequence, ozone depletion appears in the middle and upper

stratosphere due to the catalytic cycle associated with reactive NO_x. Each chemical family results in a new equilibrium, and the ozone layer appears to be 'shifted' to a lower altitude with its maximum less abundance. Due to the long lifetimes of the chlorine and bromine reservoirs in the stratosphere, the chemical perturbations caused by the BJ discharge at all studied altitudes are maintained (Xu et al., 2023, JGR-A).

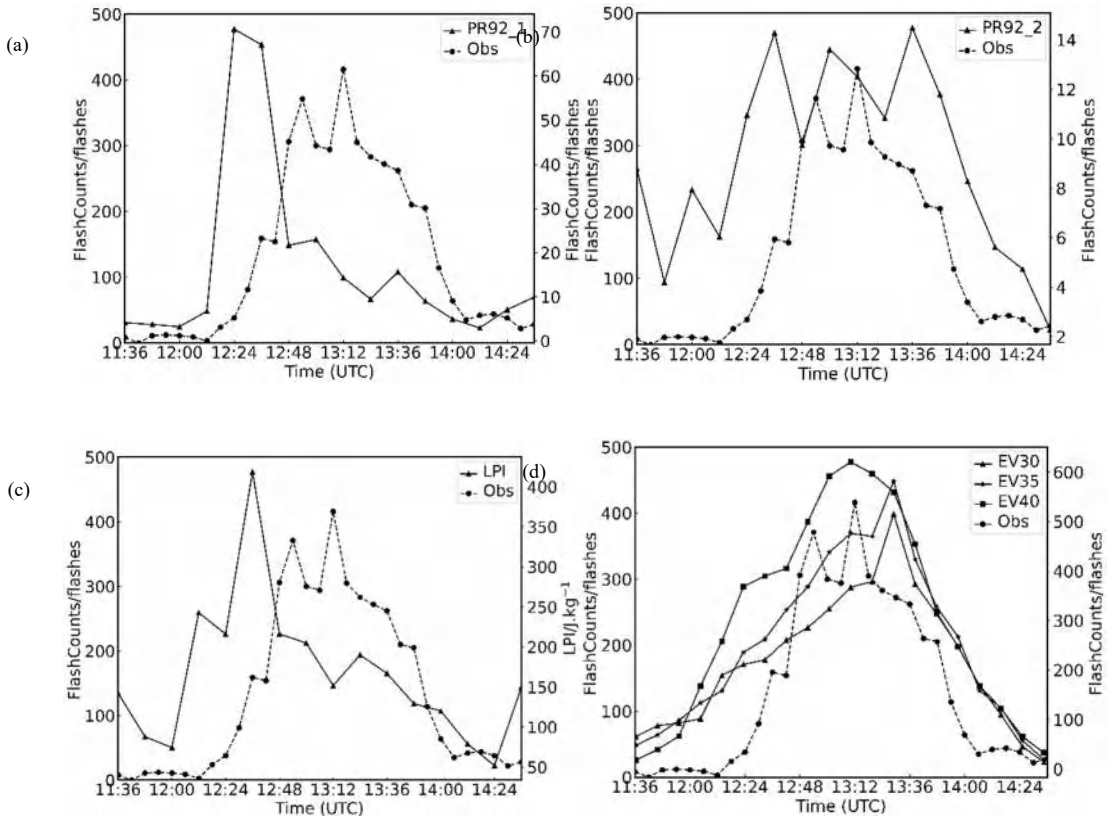

Figure 2. The temporal of the simulated lightning frequency within 12 minutes and observed lightning activity within 6 minutes of the squall line. (a) PR92_1 scheme, (b) PR92_2 scheme, (c) LPI scheme, (d) V30 dBZ scheme, V35dBZ scheme and V40dBZ scheme, the solid lines represent the simulated lightning frequency, the dotted line stands for the observed lightning frequency.

Side discharges involved in an intracloud-initiated positive cloud-to-ground lightning. In this study, utilizing fast electric field antenna, high-speed video observations, and fast antenna mapping results, we investigated positive cloud-to-ground lightning (+CG) triggered by intracloud (IC) lightning. This investigation included the initiation process of downward leaders and the subsequent leader development characteristics of positive return stroke. Below the cloud base in our field of observation, following a negative leader, three consecutive positive side breakdowns occurred beneath the horizontal main negative channel, involving

three bidirectional leaders. These bidirectional leaders advanced along the same channel, with the third leader reaching the ground, generating a positive ground flash with a peak current of 157 kA. After the positive return stroke, negative side breakdowns occurred near the vertical return stroke channel. The formed negative leader propagated outward, creating a new discharge channel, while the original return stroke channel gradually extinguished. In this lightning case, we simultaneously observed positive breakdowns along the side of the negative leader channel and negative breakdowns along the side of the positive return stroke channel, both generating branches with opposite polarities to the original channel. We propose that the phenomenon of side reverse-polarity side breakdowns in lightning channels is a crucial physical process in the initiation of positive ground flashes and represents a way for downward positive leaders to initiate on reactivated negative leader channels (Figure 3).

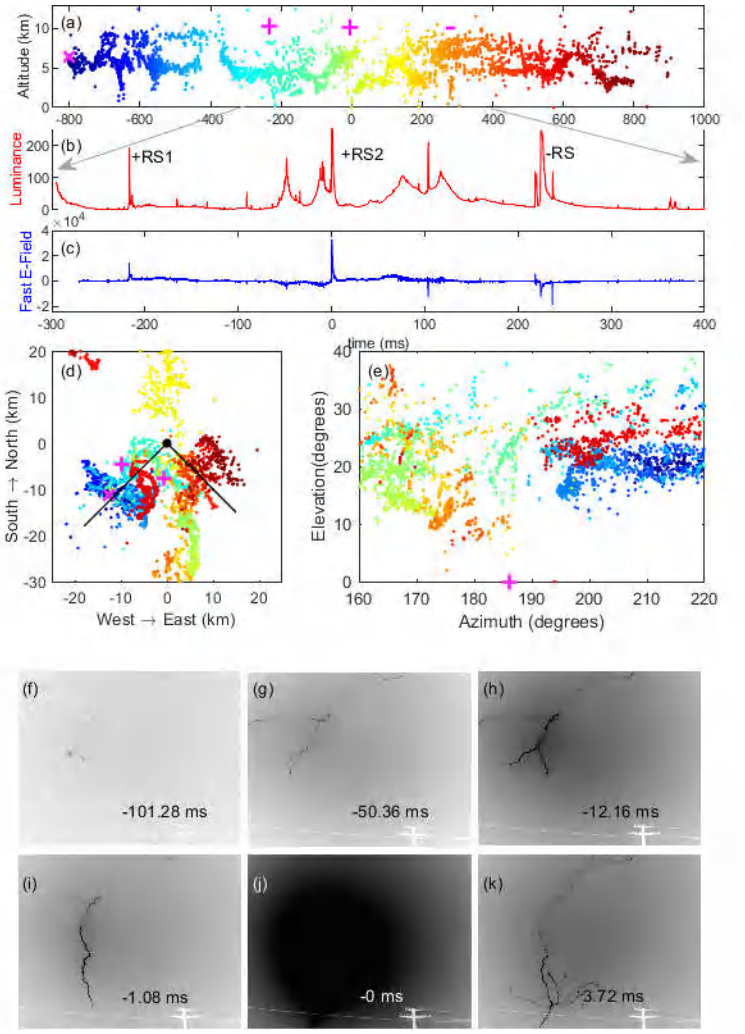

Figure 3. Dynamics of IC-Initiated +CG Lightning (0ms refers to July 10, 2021, 20:51:16.09493 UTC) (a) Height variation of fast electric field positioning results, depicted by color changes from blue to red, indicating time progression. (b) and (c) Changes in luminance intensity and fast electric

field from 300 ms before to 400 ms after the return stroke. (d) Plan view of the entire discharge process. Black dots represent observation points, and solid black lines indicate the field of view. (e) Variation of fast electric field mapping results with different viewing angles. (f-k) Optical images of the IC-initiated +CG lightning flash. Each image is labeled with time relative to the return stroke, and all images are inverted for visualization.

Israel Atmospheric Electricity Group, Reichman University, Tel Aviv University and Ariel University

Yoav Yair with Roy Yaniv (now at Hebrew University of Jerusalem) continue their analysis of PG data collected at the Wise Observatory in the Negev desert and on top Mt Hermon, in Israel. They looked at the effects of clouds, fog, and severe space weather events on the local electric field. The results were published recently. See Yaniv et al. (2023) No response of surface-level atmospheric electrical parameters in Israel to severe space weather events. Yair and Yaniv (2023) The effects of fog on the atmospheric electrical field close to the surface.

Yoav Yair is continuing the analysis of lightning and TLE data collected during the ILAN-ES experiment on board AX-1 mission to the International Space Station in April 2022. The detailed operational philosophy and the way it was conducted by Israeli astronaut Mr. Eytan Stibbe were published in *Acta Astronautica*, with the intention of helping future astronauts better understand the way of conducting successful TLE observations from the ISS Cupola window. See Yair et al. (2023) Observing lightning and transient luminous events from the international space station during ILAN-ES: An astronaut's perspective.

Colin Price, Yoav Yair, Mustafa Asfur and Jacob Silverman have published a new paper looking at the impact of sea water characteristics on lightning flash intensities. The results are based on laboratory experiments but appear to be backed up both data from super bolts over the Mediterranean Sea, and sea water samples. See Asfur et al. (2023) Spatial variability of lightning intensity over the Mediterranean Sea correlates with seawater properties.

Colin Price and graduate student Raam Bekenshtein have recently published a paper showing that deforestation over the Amazon over the past 4 decades appears to be responsible for the decrease in thunderstorm activity over the deforested regions. We explain this from the reduction in latent heat release, the decreased instability, and evapotranspiration from regions

that have been deforested. Bekenshtein et al. (2023) Is Amazon deforestation decreasing the number of thunderstorms over Tropical America?

Colin Price, graduate student Tair Plotnik, and Indian colleagues Anirban Guha and Joydeb Saha have recently published two papers looking at how lightning impacts global cirrus clouds, and also how thunderstorm changes in the Arctic may be playing a role in Arctic sea ice melting. The increasing in thunderstorms observed in the Arctic over the last decade is expected to increase the upper tropospheric water vapor, cirrus coverage and this can trap in additional IR radiation that will further warm the surface. Saha et al. (2023) The role of global thunderstorm activity in modulating global cirrus clouds. Saha et al. (2023) Are thunderstorms linked to the rapid sea ice loss in the Arctic?

Yoav Yair is now collaborating with Olivier Chanrion from DTU in the Thor-Davis experiment, being conducted on the ISS by ESA astronaut Andreas Mogensen from Denmark. The unique capabilities of the Davie camera operating at 1000 fps, ensures new imaging capabilities of TLEs and lightning from space.

Yoav Yair, Colin Price, Mustafa Asfur and Jacob Silverman had completed their research on the effects of lightning strikes on the well-being of fish in submerged cages, used for aquaculture. Results show abrupt changes of the fish school movement in conjunction with the acoustic signal from nearby lightning strokes to the sea surface. The analysis will be submitted for publication in the coming months.

Yuval Reuveni (Ariel University) and his research group continue their work on flash floods predictions using machine learning (ML) techniques applied with GPS tropospheric path delays, atmospheric pressure and lightning activity data: Asaly et al. (2023) Predicting eastern Mediterranean flash floods using support vector machines with precipitable water vapor, pressure, and lightning data.

Yuval Reuveni and his M.Sc. student, Ben Romano, have started to work on Using machine learning techniques for Geo-locating lightning activity. This study aims to explore the integration of machine learning techniques to enhance the precision and efficiency of lightning activity geo-location. Leveraging historical lightning data, meteorological variables, and advanced algorithms such as convolutional neural networks (CNNs) and recurrent neural networks (RNNs), our research aims to develop models capable of recognizing complex patterns in time-series data. Additionally, we investigate the incorporation of satellite imagery and meteorological information to refine location predictions. The study also focuses on the development of a real-time monitoring system with continuous learning capabilities.

Yuval Reuveni along with his M.Sc. student, Nadav Mauda, along with Yoav Yair continue

their work on TGEs signatures using gamma ray radiation and atmospheric electrical measurements around Mt. Hermon.

CMA Key Laboratory of Lightning, State Key Laboratory of Severe Weather, Chinese Academy of Meteorological Sciences, Beijing, China

An investigation on spatiotemporal sizes of specific types of lightning flashes. The duration and horizontal extension distance (HED) of intracloud (IC), negative cloud-to-ground (NCG), positive cloud-to-ground (PCG), and bipolar cloud-to-ground (BCG) lightning are analyzed using data from the Oklahoma Lightning Mapping Array and the National Lightning Detection Network. All of these conform to lognormal distributions. BCG lightning has the greatest average spatiotemporal size, owing to its longest-duration and largest-spatial-extension discharge process after the first return stroke (RS). Compared with NCG lightning, PCG lightning tends to include longer-duration and greater-spatial-extension discharge processes before the first RS, making the latter have a larger average spatiotemporal size. IC lightning exhibits the smallest average spatiotemporal size, with a higher concentration of samples in smaller size intervals. Overall, as lightning initiation heights increase, IC and NCG lightning duration tends to increase, while NCG lightning variation is mainly due to discharge processes before the first RS. HED of both types initially increases and then decreases, peaking at approximately 7 km. The horizontal extension speed (HES) of IC lightning tends to decrease with increasing initiation height, while for NCG lightning, the HES associated with discharge processes before the first RS shows a clearer decreasing trend at higher levels. The NCG lightning initiated below approximately 6 km tends to exhibit similar HED before the first RS and increased HED after the first RS. However, for NCG lightning initiated above approximately 6 km, the HED before the first RS is notably greater than the increased HED after the first RS.

Climatology of large peak current cloud-to-ground lightning flashes in China's most populous areas. Using a ten-year dataset of cloud-to-ground lightning (CG) flashes, the climatological characteristics of ±CG flashes with a large peak current (> 75 kA or < -75 kA) (±LPCCGs) are for the first time obtained in China's most populous areas in terms of density distribution, seasonal variation, and monthly and diurnal evolution. The results show that the distribution of +LPCCG flashes has evident

seasonal variations, while the activity center of -LPCCG flashes always remains in Southwest China (Figure 1). The diurnal evolution of +LPCCG flash percentages in southern China's Mainland shows an opposite trend to that in the north. Furthermore, the peak current distributions of +LPCCG flashes in most of China's mainland are found to be distinct from those shown in other regions of the world. Additionally, Southwest China is found to be an important and special area for LPCCG flash activity in China. Not only is it the density center of ±LPCCG flashes, but the peak current distribution of -LPCCG flashes in this region also shows an evidently different pattern from those in other regions. The diurnal evolution of the -LPCCG/+LPCCG flash frequencies in Southwest China also shows a different pattern from that in other regions.

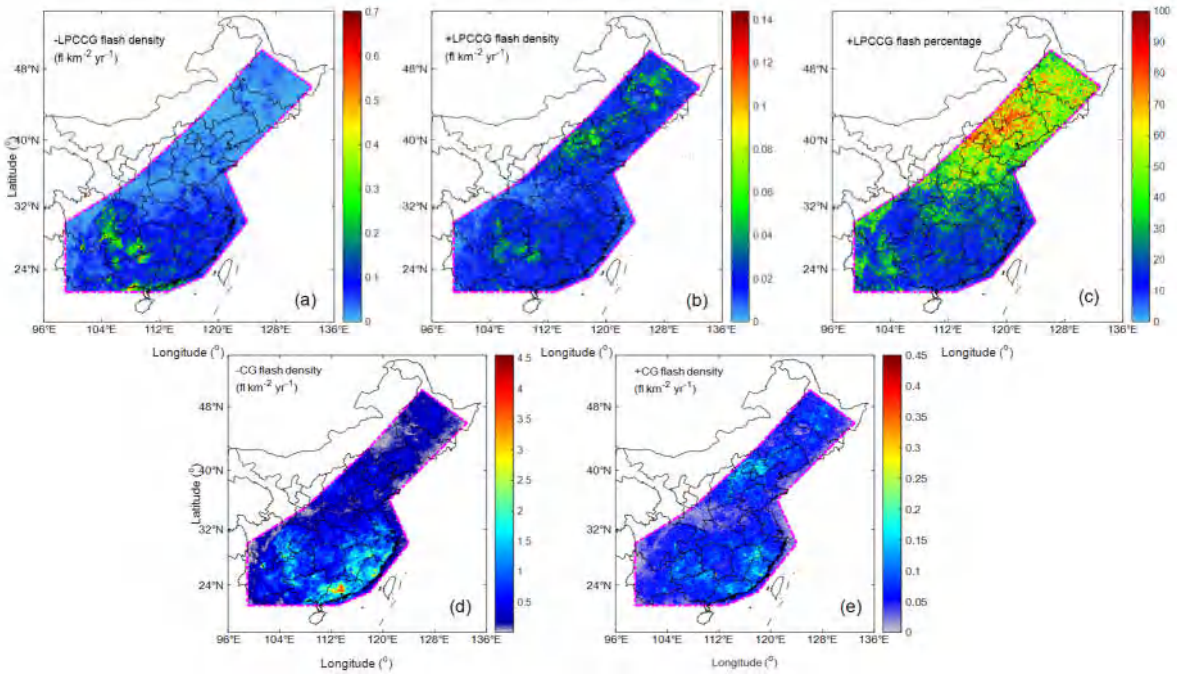

Figure 1. Distribution of the annual average (a) -LPCCG, (b) +LPCCG and (d) -CG, (e) +CG flash densities (flashes km^{-2} year^{-1}) and (c) +LPCCG percentages in the focused area from 2011 to 2020.

Correlation between frequency-divided magnetic field and channel-base current for rocket-triggered lightning. Different discharge processes of triggered lightning can radiate the electromagnetic signals with different frequency bands. During the triggered lightning experiment conducted at the Field Experiment Base on Lightning Sciences of China Meteorological Administration (CMA-FEBLS), three magnetic field (*B*-field) antennas with different frequency responses were deployed at about 80 m from the rocket launching site. By using the synchronous observations, the quantitative relationship between the close-

range *B*-field measurement and the channel-base current at different stages of triggered lightning were established in the paper. The initial continuous current (ICC) waveform can be reconstructed by numerically integrating the *B*-field signals measured with the d*B*/d*t* antenna. However, the slow variations of ICC cannot be retrieved by the *B*-field signals measured with the LF-MF antenna, because the antenna bandwidth cannot cover the frequency below 500 Hz. The *B*-field signals of return stroke measured with the low sensitivity antenna can be simulated by the MTLL return stroke model, and the *B*-field signal shows fairly good consistency with return stroke current. The analyses suggest that the current waveform of natural return stroke that occurred within 1.5 km can be retrieved or at least its peak value can be estimated by using the *B*-field measurements.

Deep convective clouds observed by ground-based radar over Naqu, Qinghai-Tibet Plateau. The deep convective clouds (DCCs, 20 dBZ echo top exceeding 14 km) and intense DCCs (IDCCs, 40 dBZ echo top exceeding 10 km) over Naqu, a city featuring the most active convection in the central Qinghai–Tibet Plateau, were analyzed on the basis of data derived from the Naqu C-band radar within a radius of 100 km. The most frequent DCCs occur in July and at 15:00 LT (local time), in terms of monthly and diurnal variations, respectively. The geographic distribution of the DCCs seems to be related to the topography. The centers featuring the most frequent DCCs correspond to some certain hilly areas, while the ratio of IDCC to DCC is greater in some specific flat areas, which may be because the hilly topography is conducive to triggering convection but is unfavorable to the full accumulation of unstable energy. The DCCs (IDCCs) have average 20, 30 and 40 dBZ echo tops of approximately 15.8 (16.5), 12.3 (14.1) and 9.9 (11.3) km, and average areas of the regions with a composite reflectivity greater than 20, 30 and 40 dBZ of approximately 120.3 (196.1), 37.4 (75.3) km^2 and 9.2 (14.6) km^2, respectively. The maximum reflectivity and horizontal extents of 20 and 30 dBZ radar echoes tend to occur at the level around –20 °C. The average horizontal extent of DCCs is much smaller than that suggested by the satellite-based radar data. In the diurnal variations in the vertical and horizontal extents of DCCs, the parameters related to 30 dBZ always increase more slowly and decrease more rapidly than those related to 20 dBZ in the afternoon, which is attributed to the generally weak convection characteristics of DCCs. The strongest convection may be at 16:00 LT in Naqu.

Guangdong Lightning Mapping Array: Errors evaluation and preliminary results. The Guangdong Lightning Mapping Array (GDLMA), as the first LMA in China, was deployed in Guangzhou, Guangdong Province, China, in November 2018 by the Chinese Academy of Meteorological Sciences and New Mexico Institute of Mining and Technology. An evaluation was conducted using Monte Carlo

and an aircraft track. The average timing uncertainty of GDLMA is 35 ns based on the distributions of reduced chi-square values. Based on the aircraft track, the average horizontal error is 13 m and the average vertical error is 41 m at an altitude of 4–5 km over the network, consistent with the Monte Carlo results. Location errors outside the network exhibit noticeable directionality. The ability to characterize lightning channels varies with different location errors. In locations that are far from the network center, only the basic structure of lightning flash can be presented, while closer to the network, the flash channel structure can be mapped well. Compared with Low-to-Mid Frequency E-field Detection Array (MLFEDA), they were generally similar in overall structure, and some lightning flash characteristics such as flash duration and coverage area exhibited consistency. However, GDLMA demonstrated better flash channel structure characterization capability, while MLFEDA performed better in processes such as leader/return strokes. In addition, based on the comparison of spatial positions of one-on-one discharge events, we found that very high frequency sources were more located ahead of low frequency sources in the direction of lightning channel development. Figure1 is our flash discharges at different distances from the station center overlain atop spatial plots of range errors (a) and altitude errors (b) at 10 km MSL (Figure 2).

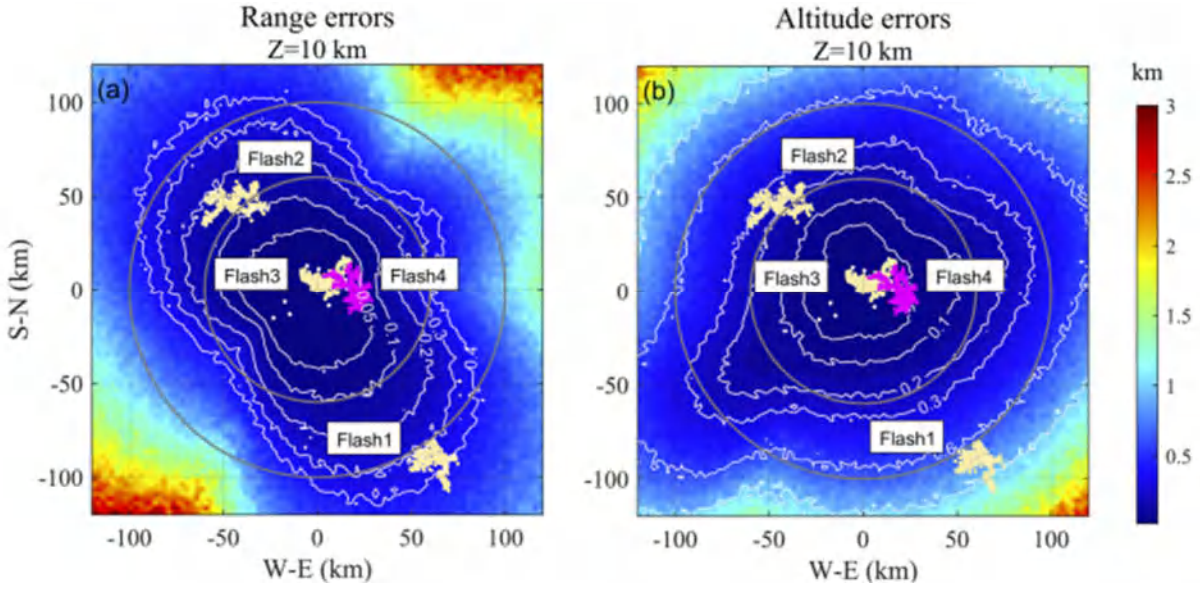

Figure 2. Four flash discharges at different distances from the station center overlain atop spatial plots of range errors (a) and altitude errors (b) at 10 km MSL. Flash 1–Flash 3 are shown in yellow and Flash 4 is shown in purple. White scatters indicate station locations and white lines are contour lines. The gray rings are 100 and 60 km from the center of Guangdong Lightning Mapping Array.

High-speed video observations of needles evolving into negative leaders in a positive cloud-to-ground lightning flash. High-speed video records of a single-stroke positive cloud-to-ground (+CG) flash were used to examine the evolution of eight needles developing more or less radially from the +CG channel. All these eight needles occurred during the later return-stroke stage and the following continuing current stage. Six needles, after their initial extension from the lateral surface of the parent channel core, elongated via bidirectional recoil events, which are responsible for flickering, and two of them evolved into negative stepped leaders. For the latter two, the mean extension speed decreased from 5.3×10^6 to 3.4×10^5 and then to 1.3×10^5 m/s during the initial, recoil-event, and stepping stages, respectively. The initial needle extension ranged from 70 to 320 m (N = 8), extension via recoil events from 50 to 210 m (N = 6), and extension via stepping from 810 to 1,870 m (N = 2). Compared with needles developing from leader channels, the different behavior of needle flickering, the longer length, the faster extension speed, and the higher flickering rate observed in this work may be attributed to a considerably higher current (rate of charge supply) during the return-stroke and early continuing-current stages of +CG flashes (Figure 3).

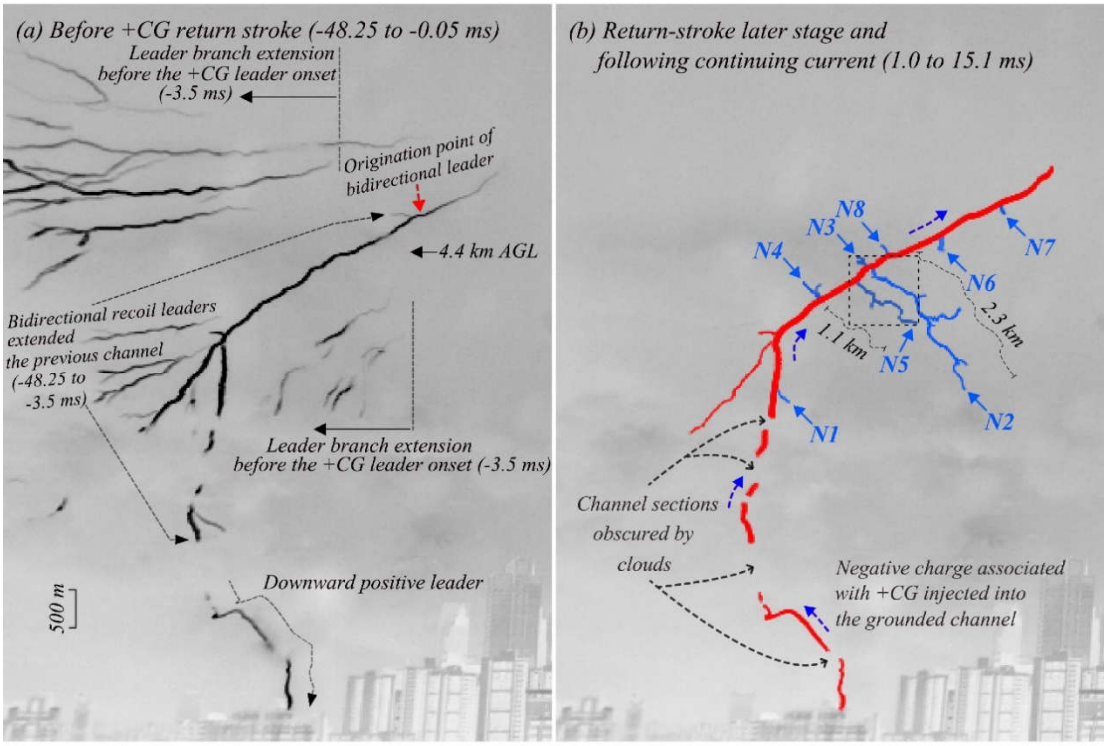

Figure 3. Composite image of 300 selected frames (from −48.25 to −0.05 ms) obtained using HC-1 camera operating at 20,000 frames per second (50-μs interframe interval), showing the overall geometry of the downward positive leader channel (positive end of the bidirectional leader tree), largely formed via a sequence of bidirectional recoil leaders. (b) Composite image of 250 selected

frames (from 1.0 to 15.1 ms) obtained using HC-1 camera (50-μs interframe interval) showing eight needles, N1 to N8, originating from the grounded channel during the return stroke (RS) and continuing current stages.

Observation and simulation of lightning strikes in an offshore wind turbine cluster. Based on the detection data of the Guangdong-Hong Kong-Macau lightning location system from 2013 to 2022, this paper analyzes the characteristics of lightning strikes in an offshore wind turbine cluster (WTC) in Guangdong. This is the first time to quantify the lightning strikes difference between the inner and outer wind turbines (WTs) and discuss the impact mechanisms of WTCs on the characteristics of lightning strikes by the simulation results of electric potential distribution. The observation results show that the stroke density, cloud-to-ground (CG) flash density, and average peak current within the affected area increase by 10.1%, 11%, and 5.1%, respectively, but the lightning multiplicity changes little. The inner and outer WTs show different characteristics of lightning strikes. The stroke density, lightning multiplicity, and average peak current in the area of outer WTs increase by 21%, 4.1%, and 6.8%, respectively, while in the area of inner WTs decrease by 20.2%, 19%, and 3.9%, respectively. The CG flash density in the area of outer WTs increases by 16.1% but changes little in the area of inner WTs. The simulation results show there is a significant difference in the electric potential distribution between the inner and outer WTs: the distortion effect of the outer WTs on spatial electric potential is stronger than that of the inner WTs at a greater height, but the difference is not obvious at a lower height. Such a difference in electric potential distribution leads to different characteristics of lightning strikes between the inner and outer WTs. Figure 4 is the average stroke density and the corresponding change rate in each sub-area during TB (the period after the installation of the WTC) and TA (the period before the installation of the WTC) periods (year^{-1} km^{-2}).

The attachment process of negative connecting leader to the lateral surface of downward positive leader in a positive cloud-to-ground lightning flash. In the lightning attachment process, the leader connecting behavior is an interesting topic. In the attachment process of a negative cloud-to-ground lightning flash, the “Tip to the lateral surface” connection type has been widely observed, and researchers have carried out a series of studies and discussions on the characteristics and the physical mechanisms of the leader connecting behavior. However, is there also a “Tip to the lateral surface” connecting behavior in the attachment process of the positive cloud-to-ground lightning flash? Using high-speed video cameras operating with framing rates of 20 and 50 kiloframes per second, we captured an attachment process during a positive cloud-to-ground flash, which demonstrates the connection of the negative

connecting leader (NCL) to the lateral surface of the downward positive leader (DPL) for the first time. When the NCL was initiated, the tip of the DPL had passed the initiation position of the NCL for about 50 m. A common streamer zone (CSZ) was observed when the three-dimensional distance between the NCL tip and the lateral surface of DPL was about 30 m. It is remarkable to note that a luminous segment (space stem/leader) with a length of about 7 m was captured within the CSZ during the attachment process (Figure 5). The connection between the NCL tip and the lateral surface of the DPL was caused by the development of the CSZ and its inner space leader.

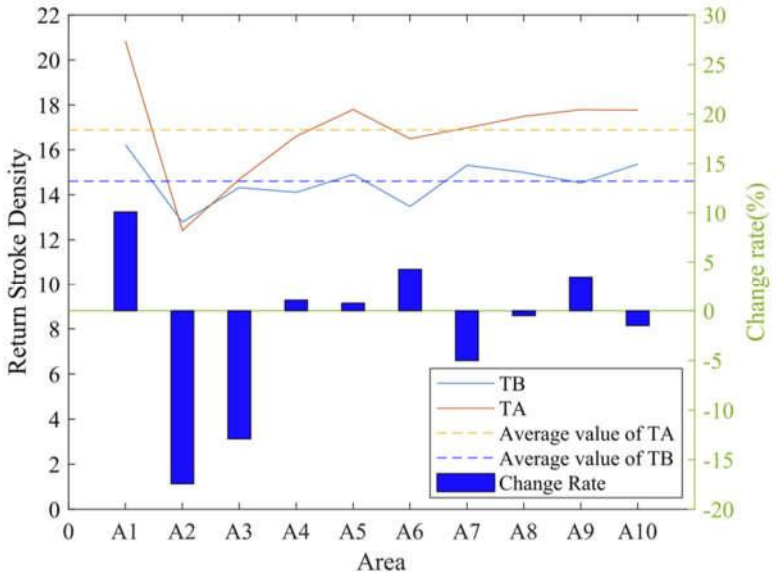

Figure 4. The average stroke density and the corresponding change rate in each sub-area during TB and TA periods (year^{-1} km^{-2}).

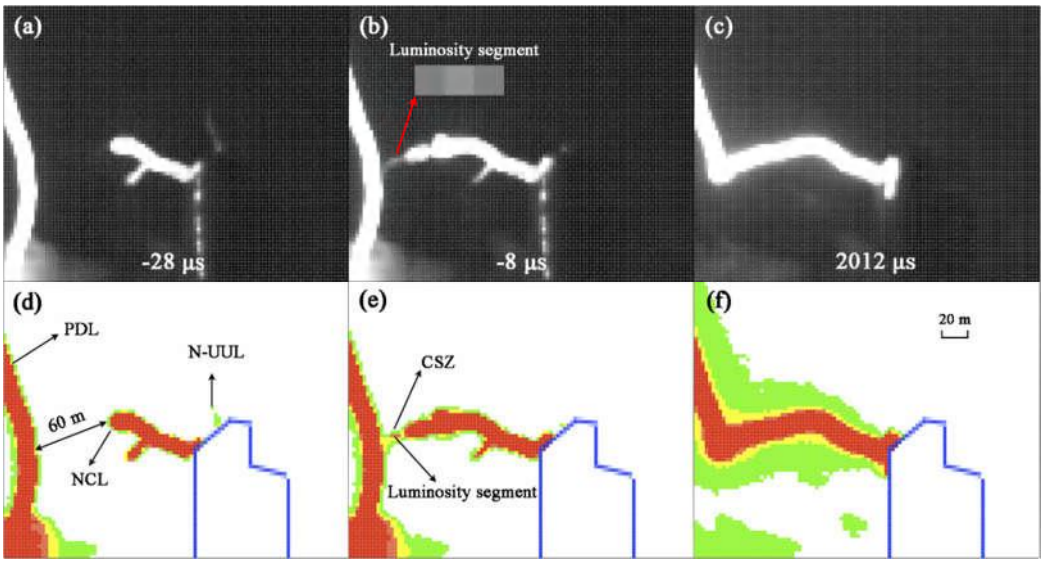

Figure 5. The last two frames (a and b) of lightning FB2101 before the return stroke and (c) the return stroke channel captured by the high-speed video camera HC-2 (50, 000 fps); (d), (e), and (f) were the

pseudo color images of (a), (b), and (c), respectively. The outline of the building was represented by solid blue lines. Time 0 was the onset of the return stroke. The exposure end time corresponding to the image was given. The original image was undergone clipping and enlarging process. In Figure (b), the luminosity segment (space leader) has also been enlarged. (DPL=Downward Positive Leader; NCL=Negative Connecting Leader; N-UUL=Negative Unconnected Upward Leader; CSZ=Common Streamer Zone).

We propose a schematic diagram of connecting behavior between positive and negative leaders during the attachment processes. Figure 6 shows the connection between the negative leader tip and the lateral surface of the positive leader, which basically includes three scenarios: (1) Before the leader connecting occurs, the downward negative or positive leader and the positive UCL or NCL are usually spatially interlaced, and the leader tips of the two different polarities already miss each other, as illustrated in Figure 6(a); (2) the distance between the negative leader tip and the lateral surface of the positive leader should be close enough to generate a CSZ (Figure 6(b2)); (3) a space stem/leader (Figure 6(c2)) is formed inside the CSZ, which develops in both directions and connects the positive and negative leaders to form a return stroke channel (Figure 6(d2)). However, it is interesting to note that no observations on the positive leader tip connecting to the lateral surface of the negative leader in natural lightning have been reported yet, which may be related to the different physical mechanisms of the development of the positive and negative leader.

Thunderstorm and lightning activities over Western Pacific, Northern Indian Ocean and South China Sea along with their adjacent lands. The Lightning Imaging Sensor (LIS) and Radar Precipitation Feature (RPF) data are used to investigate the activities and properties of lightning and thunderstorms over a region including the Western Pacific, northern Indian Ocean and the South China Sea along with their adjacent lands. The lands feature significantly more frequent lightning flashes and thunderstorms than the oceans, especially the open oceans. The highest densities of lightning and thunderstorm occur over the Strait of Malacca and the southern foothills of the Himalayas. Over the ocean regions, the Bay of Bengal and the South China Sea are characterized by relatively frequent lightning and thunderstorm activities. Larger average spatiotemporal size and optical radiance of flashes can be found over the oceans; specifically, the offshore area features the most significant flash duration, and the open ocean area is characterized by the greatest flash length and optical radiance. The smallest average values of flash properties can be found over and around the Tibetan Plateau (TP). The oceanic thunderstorms tend to have a significantly larger horizontal extent than the continental thunderstorms, with the former and latter having

the average area of the regions with radar reflectivity larger than 20 dBZ, generally over 7000 km^2 and commonly below 6000 km^2, respectively. The TP thunderstorms show the smallest horizontal extent. Meanwhile, the oceanic thunderstorms exhibit greater 20 dBZ but smaller 40 dBZ top heights than the continental thunderstorms. The average flash frequency and density of the oceanic thunderstorms are typically less than 5 fl min^{-1} and 0.3 fl 100 km^{-2} min^{-1}, respectively; in contrast, the corresponding values of continental thunderstorms are greater. It is explored that the regions associated with strong convective thunderstorms are more likely to feature small-horizontal-extent and low-radiance flashes.

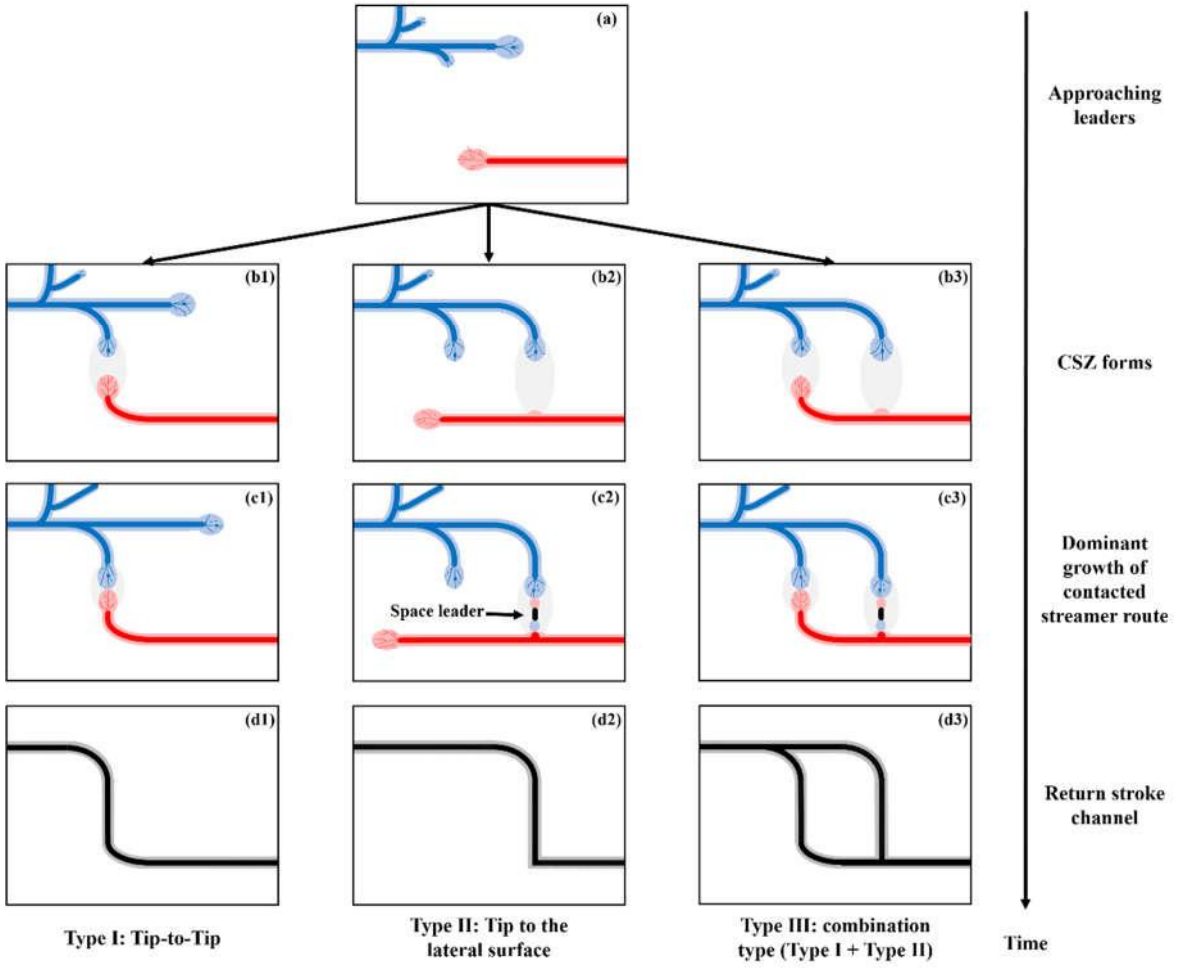

Figure 6. Schematic diagram of connecting scenarios between positive and negative leaders: (a) the positive and negative leaders are staggered in space, (b1) to (d1) the negative leader tip connected to the positive leader tip (Type I), (b2) to (d2) the negative leader tip connected to the lateral surface of the positive leader (Type II), and (b3) to (d3) combination of Type I and Type II (Type III).

Lightning Research Group of Gifu University (Gifu, Japan)

A simple and accurate method based on the random forest classifier to classify return stroke radiation waveforms. We developed a simple machine-learning classifier for radiation waveforms of negative return strokes (RSs) based on the Random Forest classifier. The classifier was built and tested using a large dataset consisting of 14,898 negative RSs and 159,277 intracloud (IC) pulses with 3-D location information. Because of the 3-D location information, we can almost unambiguously discriminate RSs and thus can have a high-quality dataset for learning and testing. The classifier is very simple to build; it only requires eleven parameters that can be easily calculated based on the waveforms. These parameters are illustrated in Figure 1. They include three parameters related with pulse characteristics and eight parameters related with the relative strength of pulses. We also defined two parameters for the evaluation of the classifier performance, including the *classification accuracy*, which is the percentage of true RSs in all classified RSs, and the *identification efficiency*, which is the percentage of correctly classified RSs in all true RSs. The tradeoff between the accuracy and the efficiency is examined and simple methods to tune the tradeoff are developed.

The classifier achieved the best overall performance with an accuracy of 98.84% and an efficiency of 98.81%. With the same technique, the classifier for positive RSs is also built and tested using a data set consisting of 8,700 positive RSs. The classifier has an accuracy of 99.04% and an efficiency of 98.37%. By examining misclassified waveforms, we show evidence that some RSs and IC discharges produce special radiation waveforms that are almost impossible to correctly classify without 3-D location information, resulting in a fundamental difficulty to achieve very high accuracy and efficiency in the classification of lightning radiation waveforms. This study has been published in JGR: Atmospheres. A simple Python script to use the classifiers is also provided with the paper.

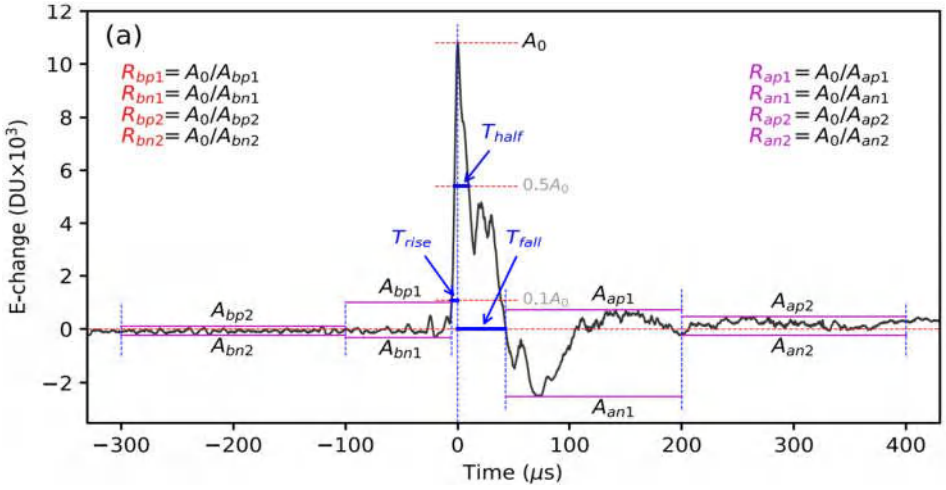

Figure 1. Illustration of waveform parameters based on a return stroke pulse.

Massachusetts Institute of Technology

Earle Williams

Earle Williams is about 2/3 complete on a generous 3-month Visiting Research Fellowship to Sopron, Hungary. This visit has involved an invited talk on Lightning and Climate Change at Eötvös Lorand University in Budapest, and the engagement in a number of research topics with Hungarian collaborators Gabriella Satori, Jozsef Bor, Erno Pracser, Tamas Bozoki and Daniel Piri. Short summaries of these various topics are noted below:

(1) Impact of polar outbreaks on global lightning. Given the discovery of a simultaneous outbreak from both poles in the period January 16-20, 2019, we returned to this topic with Matyas Herein (Eötvös Lorand University), Tamas Bozoki and Gabriella Satori to make a short presentation at the recent NASA GLM Science Meeting. Geostationary Lightning Mapper showed that the Western Hemisphere lightning total declined by more than a factor-of-two during this event. Diminishments in temperature, moisture and aerosol linked with the polar air have been suggested as possible explanations. Herein is exploring models to access the probability of simultaneous events from both poles. The impacts of these events on the DC global circuit is also of interest.

(2) High voltage transmission lines for air-earth current measurements. Unused lines have been identified in the Sopron, Hungary area by Jozsef Bor and Ferenc Varga for tests in the capture of the fair-weather air-earth current of the DC global circuit, over larger areas than available in previous measurements. Extensive calculations have also been made of the capacitive coupling effect of neighboring active lines on the unused lines. The NanoRanger digital nano-ammeter has been identified as a useful and inexpensive ($200) instrument for tests of the DC current to ground. Its bandpass characteristics have been studied by Daniel Piri.

(3) High latitude perspective on Schumann resonances. Polar monitoring of near-equatorial lightning "chimneys" serves to fix the source-receiver distance for lightning sources and greatly simplifies the quantitative interpretation of Schumann resonances and the ranking of three chimneys on individual days. Observations from high latitude stations Hornsund at Spitsbergen (operated by Mariusz Neska) and Maitri in Antarctica (operated by Ashwini, Sinha, Rahul Rawat, Geeta Vichare, and Jeeva Krishnamurthy) are used as approximations for the Schumann resonance response at the South Pole where an installation is planned pending NSF support. Excellent agreement is found in the relative variation in chimney strengths as seen from the two locations.

(4) South American squall lines as well-defined lightning sources. In the interpretation

of Schumann resonance frequency variations, one needs information on the motion of lightning sources relative to nodal boundaries along great circle paths. Long squall lines in South America are good candidates for observations of the vertical electric field from Nagycenk Observatory in Hungary. Rachel Albrecht and Raidiel Puig at the University of Sao Paulo have provided hourly GLM lightning observations on squall line days to shed important new light on this problem. The lightning observations delineate the squall line positions and motions much better than satellite VIS/IR observations, and/or TRMM precipitation radar observations.

(5) Continuing current assessment in lightning initiation of forest fires. Continuing current with time constants an order-of-magnitude longer than typical return stroke durations in lightning flashes is recognized as a spectral reddening agent for Schumann resonance background spectra. The long duration of the continuing current is also recognized as essential for the initiation of forest fire, largely on the basis of earlier laboratory observations by Don Latham. Scott Rudlosky (NASA MSFC) presented observations linking specific lightning flashes with the initiation of specific forest fires at the recent GLM Science meeting. Janusz Mlynarczyk will deploy wideband ELF methods to identify and characterize the continuing current in single-stroke flashes of both polarities that have been shown to initiate forest fire.

The inexpensive electric field sensor designed by Ken Cummins and slated to be used in the measurement of the ionospheric potential of the DC global circuit continues to be improved at Quasar Federal Systems (Yongming Zhang) in San Diego. An AGU poster updating this work is in production. An additional field test is tentatively planned for January 2024.

Bill Koshak and Ken Cummins presented interesting evidence at the GLM Science meeting for a decadal decline in NLDN-recorded cloud-to-ground lightning. Wolfgang Schulz has pointed out similar declines in Europe (Germany and Austria). This consistent behavior has motivated speculation on the possibility of long-term changes in the IC/CG ratio, with more IC lightning and less CG lightning in a warmer climate.

Ashot Chilingarian has recently published a Comment in JGR (Chilingarian et al., "TGE electron energy spectra: Comment on "Radar diagnostics of the thundercloud electron accelerator"" by E. Williams et al. (2022), 2023) on our earlier study in Armenia, and focused on issues of Compton electrons and the observational evidence for free passage distances less than 100 meters. An expanded study on these issues is now in press at JGR (Williams et al., "Conditions for energetic electrons and gamma rays in thunderstorm ground enhancements" 2023).

Netherlands LOFAR Lightning Group

The group at the University of Groningen, and ASTRON, Netherlands, has been active using the LOFAR radio telescope to image lightning in VHF (30-80 MHz) at the highest resolutions. In one recently published work [1] we have invested the structure of intracloud dart leaders (referred to as recoil leaders in the publication). Figure 1 demonstrates two of the major findings of this work.

Firstly, the left-panel of Figure 1 shows the difference between the locations of VHF sources and a smoothing spline along two dart leaders, in the radial direction from LOFAR's core (worst located coordinate). This figure shows that most VHF sources are within a tightly packed core. A Gaussian function fitted to the locations of sources within 10 m of the spline (to exclude the long tail of miss-located sources), has a standard deviation of 1.8 m. This width is consistent with imaging and spline-fitting inaccuracies. The conclusion is that dart leaders are thinner than a meter when viewed in VHF. Since we suspect that VHF is emitted by streamer activity (see refs. in [1]), the possible physics interpretation is that the majority of dart leader streamer activity is confined to near/inside of the leader core and not extending out into the corona sheath (which is thought to be 10 m wide at minimum, see refs. in [1]). Secondly, the right panel of Figure 1 shows the VHF power emitted by the same two dart leaders vs their propagation speed in a log-log scale. This plot shows the surprising result that the VHF energy emitted by a dart leader is either power-law or logarithmically related to the speed of the dart leader.

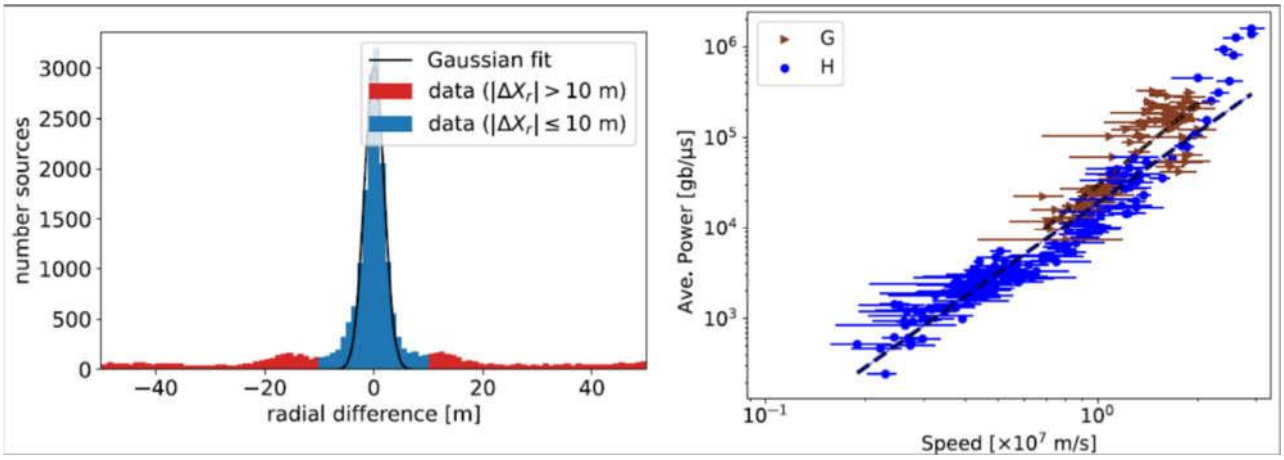

Figure 1. Two major results of [1]. LEFT: The difference in position (in radial direction) between VHF source locations and a smoothing spline, of two dart leaders. The fitted Gaussian has a standard deviation of 1.8 m. RIGHT: The VHF power vs speed of the same two intracloud dart leaders, on a log-log scale. Figure adapted from [1].

We have extensively studied phenomena that occur along positive leaders (i.e. needles and dart leaders) but have so far been unable to image the tip of a positive leader in VHF. Therefore, in [2] we actively searched for the tip of a positive leader using our most sensitive beamforming imager that, through coherent summation of signals, is able to probe amplitude levels far lower than noise-floor of a single antenna. However, even with such a sensitive technique we were unable to locate a positive leader tip. Instead, set an upper limit for the energy emitted by a positive leader at 60 MHz to be 0.5 pJ/MHz. In future work we will attempt to image lightning with significantly more antennas. Since positive leaders have been observed in VHF near ground (see refs. in [2]), we speculate that perhaps the VHF emitted power from positive leaders may also be related to their propagation speed (inspired by the results of [1]). Thus, faster propagating positive leaders tips may be easier to locate in VHF.

In another work we investigated small VHF-emitting structures that we observe near the top of intense thunderstorms, that do not seem directly connected to a fully-developed lightning flash [3]. Due to their small-size, we refer to these phenomena as sparkles. Figure 2 shows many seemingly-disconnected VHF sources above 10 km altitude. One of the sparkles is large enough that it resembles a small lightning flash. It is possible that these sparkles are related to BLUEs observed by ASIM (see refs. in [3]). The sparkles are not uniformly distributed throughout the cloud, but appear close together in layers. This raises the question if the sparkles are truly independent, or some of them are connected with VHF-invisible positive leaders. On closer inspection, the sparkles come in great variety. Some of them appear as a collection of only 2-3 located sources. While others clearly show a developed negative leader, and sometimes even a dart leader. Thus, it is likely that sparkles (and perhaps BLUEs by extension) are not one phenomena, but multiple related types of small discharges. Two questions of interest to our group being: why do the sparkles appear near the top of the cloud? (as opposed to deeper where larger flashes tend to initiate), and why do the sparkles seem to cluster together in groups and layers?

In order to better assist in search LOFAR lightning images for phenomena of interest, we have explored the possibility of applying machine learning techniques to LOFAR images [4]. This work included using a TNSE algorithm coupled with a clustering algorithm to attempt to separate a lightning flash into distinct categories (primarily negative leaders, dart leaders, and needles). The results show promise, but more work is needed.

[1] B. M. Hare, O. Scholten et al. "*Characteristics of recoil leaders as observed by LOFAR*", *Phys. Rev. D*, vol. 107, pg. 023025, doi: 10.1103/PhysRevD.107.023025.

[2] O. Scholten, B.M. Hare et al. "Searching for intra-cloud positive leaders in VHF",

*Scientific Report*s, vol 13, article num. 14485, doi: 10.1038/s41598-023-41218-x.

[3] O. Scholten, B.M. Hare et al. "Small-scale discharges observed near the top of a thunderstorm", *Geophysical Research Letters*, vol. 50, pg. E2022GL101304, doi: 10.1029/2022GL101304.

[4] L. Wang et al. "Identifying lightning structures via machine learning", *Chaos, Solitons & Fractals*, vol. 170, pg. 113346, doi: 10.1016/j.chaos.2023.113346.

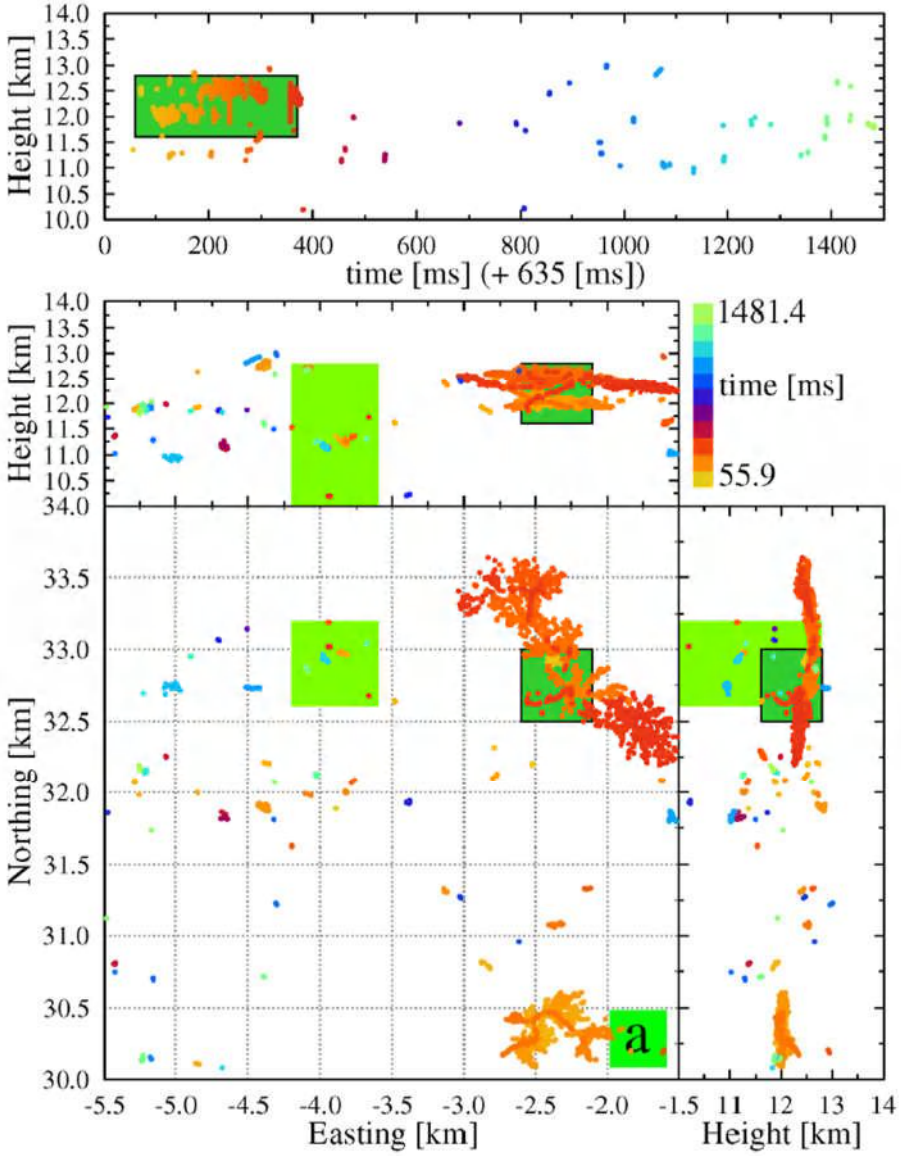

Figure 2. Sparkles seen by LOFAR, including one of significant size. The green boxes show areas that are zoomed-in to in the full paper. Adapted from [3].

Northwest Normal University, China

The propagation characteristics of the return-stroke electric wave in consideration of corona sheath. The propagation characteristics of the return-stroke current wave along the channel are an important issue in lightning research. The temperature, electrical conductivity and radius of lightning dart leader channels were calculated based on spectral diagnosis. Using them as initial parameters the dispersion equation for electric wave propagating along the return-stroke channel in a wide angular frequency range was solved numerically. The dispersion relations for the electric wave with and without considering the corona sheath effect were investigated. The results showed that both the propagation velocity and amplitude of electric wave decay along the channel, and the high frequency components decay faster. The corona sheath hastens the attenuation of the electric wave, as shown in Figure 1. Since the peak current intensity is closely related to the physical characteristics of the leader channel and determines the propagation velocity and amplitude attenuation of electric wave. Inferred from the attenuation characteristics of the wave, the variation of the current intensity along the channel is mainly determined by the different attenuation rate of the harmonic components with different frequencies during the transmission process.

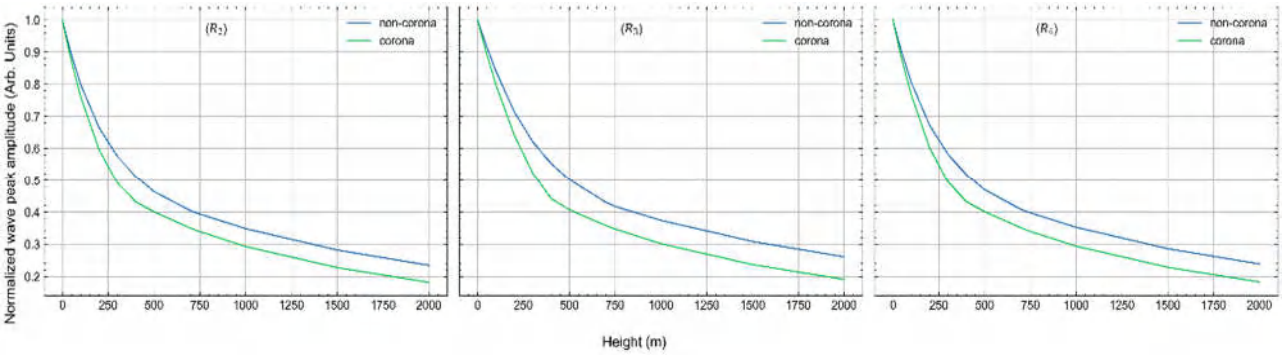

Figure 1. The amplitudes of electric wave peaks versus channel height.

Time-evolution characteristics of spectrum and temperature of lightning discharge plasma. Temperature is one of the crucial parameters reflecting the energy and current transfer characteristics in lightning discharge plasma channel. According to the spectra of lightning return strokes discharge recorded simultaneously by two high-speed slit-less spectrographs with different time resolutions, the spectral intensity and temperature evolution of the plasma channels over time was quantitatively analyzed. The spectral characteristics show that the intensity of ionic lines decayed rapidly with time as the discharge

current declined, while that of the atomic lines decreased more slowly. Additionally, it is found that the ionic lines existed for much longer time than previously reported values, up to hundreds of microseconds in the spectra of continuing current process. It further indicates that the ionic line intensities are associated with the discharge currents and that their radiation mechanism is closely related to the collision excitation under the action of strong currents. The temperature calculated by the ionic lines can reflect the thermodynamic properties of the current-carrying channel. The temperature calculated using atomic lines is significantly lower than that calculated by the ionic lines in the same spectrum. The radiation mechanism for majority of the atomic lines should differ from that of the ionic lines. During the continuing current, the channel temperatures calculated by both ionic lines and atomic lines showed a similar evolution feature which declined slowly or even basically unchanged. This property reflects the persistent heating effect of the discharge current.

University of Florida

Z. Ding, V. A. Rakov, Y. Zhu, I. Kereszy, S. Chen, and M. D. Tran authored a paper titled "Propagation mechanism of branched downward positive leader resulting in a negative cloud-to-ground flash". Our basic knowledge of downward positive lightning leaders is incomplete due to their rarity and limited ability of VHF mapping systems to image positive streamers. In this paper, using high-speed optical records and wideband electric field and magnetic field derivative signatures, the authors examined in detail the development of a descending positive leader, which extended intermittently via alternating branching at altitudes of 4.2 to 1.9 km and involved luminosity transients separated by millisecond-scale quiet intervals. They have shown that the transients (1) are mostly initiated in previously created but already decayed branches, at a distance of the order of 100 m above the branch lower extremity, (2) extend bidirectionally with negative charge moving up, (3) establish a temporary (1 ms or so) steady-current connection to the negative part of the overall bidirectional leader tree, and (4) exhibit brightening accompanied by new breakdowns at the positive leader end. One of the transients unexpectedly resulted in a negative cloud-to-ground discharge. Both positive and negative ends of the transients extended at speeds of 10^6 to 10^7 m/s, while the overall positive leader extension speed was as low as 10^3 to 10^4 m/s. Wideband electric field signatures of the transients were similar to K-changes, with their millisecond- and microsecond-scale features being associated with the steady current and new

breakdowns, respectively. For transients with both ends visible in the optical records, charge transfers and average currents were estimated to be typically a few hundreds of millicoulombs and some hundreds of amperes, respectively. The paper is published in the Journal of Geophysical Research – Atmospheres doi:10.1029/2023JD039262.

K. Kutsuna, N. Nagaoka, Y. Baba, T. Tsuboi, and V.A. Rakov authored a collaborative paper titled "Estimation of lightning channel-base current from far electromagnetic field in the case of inclined channel". The authors have derived mathematical expressions to estimate the peak and waveshape of lightning return-stroke current at the channel base from the waveform of electromagnetic field observed more than some tens of kilometers away from an inclined lightning channel. Three models of the lightning return stroke were considered, the transmission-line (TL) model, the modified TL model with linear current decay with height (MTLL), and the modified TL model with exponential current decay with height (MTLE). The peak of the lightning return-stroke current at the channel base was estimated from the peak of observed lightning electric or magnetic field using an analytical relation between the peak of channel-base current and that of the radiation field component for an inclined channel. The waveform of the channel-base current was reconstructed from the electric or magnetic field waveform using a relation between the channel-base current and the sum of induction and radiation field components for an inclined channel. It has been shown that the peak and waveshape of current at the base of an inclined channel are sufficiently accurately estimated with the proposed expressions. This work is the first attempt to solve the inverse problem (infer source parameters from electromagnetic fields) for the case of inclined lightning channel. Solving this problem is important for developing methodology of remote measurements of lightning currents. The paper is published in the Electric Power Systems Research (EPSR).

University of Science and Technology of China

Low frequency magnetic field observations of natural positive leaders featuring stepwise propagation. The low-frequency (LF) magnetic pulses were recorded for the positive leader in two natural lightning flashes captured by the high-speed video camera. The captured positive leader in both cases propagated in a stepwise manner at least over several milliseconds according to the concurrent sequence of LF magnetic pulses. By comparing with previous studies on positive leaders under different situations, the average inter-pulse intervals (11.7 and 20.3 μs, respectively) obtained for our natural cases are shorter than that of upward

positive leaders in rocket-triggered (typically >25 μs) and tower-initiated lightning (62 μs in one case). Hence, the stepwise propagation of positive leaders in natural lightning is likely more frequent than that in object-induced lightning, reflecting a possible influence of ambient electric field and other meteorological factors on the stepwise feature of positive leader. The stepwise extension might be common for positive leaders developing in various scenarios. For more detailed results, please visit doi:10.1029/2023GL105540.

Spatiotemporal patterns of long series of cloud-to-ground lightning in Beijing and its cause. The long series of lightning location data during 2009–2018 were applied to reveal the spatiotemporal distribution of cloud-to-ground (CG) lightning in Beijing. The spatial characteristics were low west and high east, and the temporal characteristics were frequent in summer. In the complex terrain areas of northeast Beijing, there was a positive relationship between CG density and altitude, with the correlation coefficient higher than 0.8. The northeastern trumpet-shaped terrain had the forced lifting effect on thunderstorms, forming lightning-intensive areas of 500 km^2. In addition, urban heat island (UHI) effect provided the necessary thermal conditions for the development of thunderstorms, forming lightning-intensive areas in the built-up areas, with the highest value of CG flash density exceeding 6 fl/km^2. Note that the lightning-sparse areas in the urban center exhibited a distinct barrier effect on the spatial patterns of summertime CG lightning in the built-up areas, which was mainly modulated by the type of synoptic background. For more detailed results, please visit doi:10.1016/j.uclim.2023.101480.

A comparative study on the electrical characteristics of positive and negative narrow bipolar events. Narrow bipolar events (NBEs) are one sort of intriguing intra-cloud discharges that receive enormous interest in the lightning community. They come with two polarities dominating at different altitudes in thunderclouds. NBEs may occur at the onset of lightning, but the electrical properties of NBEs remain not well understood. Here, we present a comparative study on the electrical characteristics of negative and positive NBEs. An improved method based on the transmission line model is applied to derive electrical parameters from the fast electric field change waveforms of 1673 positive NBEs and 364 negative NBEs recorded by the Jianghuai Area Sferic Array (JASA) in China. It is found that negative NBEs occurring at high altitudes tend to produce a narrower current pulse and take a shorter time to traverse the channel than their positive counterparts. Moreover, a larger portion of negative NBEs is associated with slightly greater peak current moment but smaller overall charge moment compared to their positive counterparts. For more detailed results, please visit doi:10.1016/j.uclim.2023.101480.

Automatic recognition of tweek atmospherics and plasma diagnostics in the

lower ionosphere with the machine learning method. Tweek atmospherics are extremely low frequency and very low frequency pulse signals with frequency dispersion characteristics that originate from lightning discharges and that propagate in the Earth–ionosphere waveguide over long distances. In this study, we developed an automatic method to recognize tweek atmospherics and diagnose the lower ionosphere based on the machine learning method. The differences (automatic − manual) in each ionosphere parameter between the automatic method and the manual method were −0.07 ± 2.73 km, 0.03 ± 0.92 cm−3, and 91 ± 1,068 km for the ionospheric reflection height (*h*), equivalent electron densities at reflection heights (*N*e), and propagation distance (*d*), respectively. Moreover, the automatic method is capable of recognizing higher harmonic tweek sferics. The evaluation results of the model suggest that the automatic method is a powerful tool for investigating the long-term variations in the lower ionosphere. For more detailed results, please visit doi:10.26464/epp2023085.

Quantitative relationship between current pulses and associated low-frequency magnetic fields during initial stage of rocket-triggered lightning. The quantitative relationship between the channel-base current and the associated low-frequency magnetic field (*B*-field) during the early stage of rocket-triggered lightning was examined based on field experiments and numerical simulation. There is a good correlation between the current pulse and the corresponding *B*-field pulse in terms of amplitude and duration. In specific, the duration of current pulse is approximately proportional to that of the corresponding *B*-field pulse for precursors and initial upward leaders; as for the pulse amplitude, the linear correlation is more apparent for the initial upward leaders when compared to the precursors, with the ratio of *B*-field pulse and current pulse between 1.7 and 2.0, which is always greater than that (0.97–1.32) for the precursors. A response function is established to show the quantitative relationship in the time domain between the current pulse and the associated *B*-field pulse, which is considered as the convolution of the current pulse and the response function. Meanwhile, the current waveform can be obtained if the measured *B*-field pulse is de-convolved with the response function. The simulation results are in good agreement with the measurement, which proves that our approach is accurate and efficient to quantify the relationship between the current and the *B*-field pulse of the initial leader discharges. For more detailed results, please visit doi:10.1029/2022RS007647.

University of Texas at Dallas

Studies of the response of the global electric circuit to solar activity, and its effect on weather and climate are continuing at the University of Texas at Dallas, with Prof. Tinsley continuing to analyze data in his retirement, with publications in 2022 and 2023.

There are clear and unambiguous correlations of cloud cover and surface pressure with day-to-day changes in ionospheric potential and cosmic ray flux affecting the ionosphere-earth current density J_Z. However, the details by which the resulting space charge generated in stratiform clouds affects cloud opacity remain uncertain. There is a need for detailed observations of charge and size distributions of aerosol particles and droplets in clouds, and for comprehensive models of the cumulative effects over days of space charge generation and in-cloud mixing, and the resulting electro-anti-scavenging and electro-scavenging. These uncertainties were detailed in a JGR paper in 2022.

There are clear correlations of cloud cover and atmospheric circulation changes with the 11-year solar cycle, but correlations alone do not distinguish between hypothesized forcing by solar ultraviolet, energetic particle precipitation, or solar wind electric field inputs. In the 2023 BAMS paper "Solar Activity, Weather and Climate: The Elusive Connection" in press, Tinsley discusses the variety of evidence for the various mechanisms and concludes that the effect of J_Z on clouds is the most plausible.

There is also evidence for 22-year climate cycles and 22-year cycles in the solar wind electric field and in J_Z, and this is the subject of ongoing analysis. As with the day-to-day correlations alone, these correlations on the bi-decadal timescale allow discrimination between the UV, energetic particle and J_Z mechanisms.

Wuxi University, China

Effects of positive corona on upward leader initiation from tall building by 3D numerical simulation. The initiation of the stable upward leader (SUL) is an important criterion to judge whether a building can be struck by lightning. The corona layer above the tip of a building caused by thunderstorm will affect upward leader initiation; however, there are few studies on the degree of its specific impact. Therefore, based on the established three-dimensional corona discharge model (Guo et al., 2022) and the dynamic critical length criterion of initial streamer as reported by Guo et al. (2020), we establish an SUL initiation model with corona discharge at the tip of the tall building. It is found that the simulated results of our model

(considering corona discharge) match well with actual observations (Table 1). The model is then used to simulate buildings with different height and different peak current of lightning strike (IP). The effect of positive corona discharge at the tip of the building on the initiation of the positive SUL during downward negative cloud-to-ground flash is discussed. The results show the following: 1) for certain IP values, the effect of corona discharge at the tip of the building has a greater effect on taller buildings than shorter ones. 2) For buildings of the same height, as Ip decreases, the effect of corona discharge at the tip of the building becomes greater. For example, for an IP of 20 kA and an Hb of 200 m, at the moment of the SUL initiated from the building, the height of the DL tip above the ground is 550 m when the corona layer is considered in the simulation and is 861 m when which is not considered (Figure 1). The difference between them have reached at 36%. This study has been published in Atmospheric Research.

Table 1. The height of the leader tip above the ground (Z_0) and relative error at the moment of SUL initiation in different environments.

Compare the results	The height of Z_0 when the stable leader initiated/m	Error/%
Observations	710	/
DCLCIS (Guo et al., 2020)	665	6.33
Case 1: without E_b and corona discharge	649	8.59
Case 2: with E_b and without corona discharge	924.1	30.15
Case 3: with E_b and corona discharge	721.1	1.56

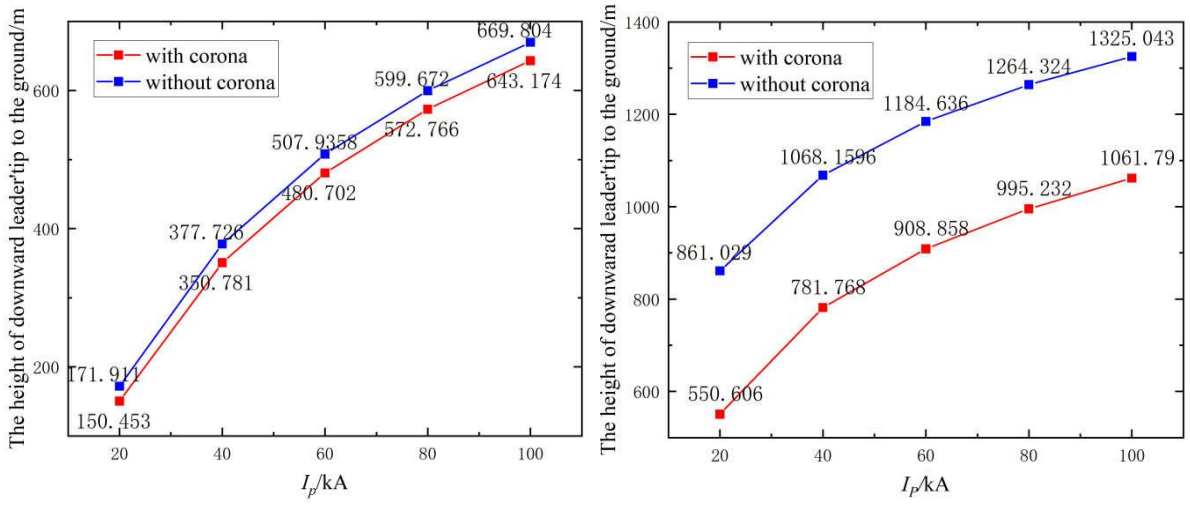

Figure 1. Comparison plot of Z_0 when SUL initiates under different I_P values and H_b values of (LEFT) 50 m and (RIGHT) 200 m.

RECENT PUBLICATIONS

This list of references is not exhaustive. It includes only papers published during the last six months provided by the authors or found from an on-line research in journal websites. Some references of papers very soon published have been provided by their authors and included in the list. The papers in review process, the papers from Proceedings of Conference are not included.

Abbasi, R.U., Saba, M.M.F., Belz, J.W., Krehbiel, P.R., Rison, W., et al. 2023. First high-speed video camera observations of a lightning flash associated with a downward terrestrial Gamma-Ray flash. Geophys. Res. Lett., 50. doi:10.1029/2023GL102958.

Asaly, S., Gottlieb, L., Yair, Y., Price, C., Reuveni, Y. 2023. Predicting eastern mediterranean flash floods using support vector machines with precipitable water vapor, pressure, and lightning data. Remote Sens., 15. doi:10.3390/rs15112916.

Asfur, M., Price, C., Yair, Y., Silverman, J. 2023. Spatial variability of lightning intensity over the Mediterranean Sea correlates with seawater properties. Scientific Reports, 13, 5834. doi:10.1038/s41598-023-33115-0.

Bahari, N., Mohammad, S., Esa, M., Ahmad, M., Ahmad, N., et al. 2023. Analysis of lightning flash rate with the occurrence of flash floods and hailstorms in Peninsular Malaysia. J. Atmos. Sol.-Terr. Phy., 250. doi:10.1016/j.jastp.2023.106121.

Bang, S.D., Stough, S.M., Lang, T.J., Gatlin, P.N. 2023. The Multiplatform Precipitation Feature (MPF) database: A storm-centric synthesis of space- and ground-based precipitation and lightning data sets for convective studies. Earth Space Sci., 10. doi:10.1029/2023EA003137.

Bekenshtein, R., Price, C., Mareev, E. 2023. Is Amazon deforestation decreasing the number of thunderstorms over Tropical America? Q. J. Roy. Met Soc., doi: 10.1002/qj.4518.

Bestard, D., Coulouvrat, F., Farges, T., Mlynarczyk, J. 2023. Acoustical power of lightning flashes. J. Geophys. Res. Atmos., 128. doi:10.1029/2023JD038714.

Bór, J., Bozóki, T., Sátori, G., Williams, E., Behnke, S. A., et al. 2023. Responses of the AC/DC global electric circuit to volcanic electrical activity in the Hunga Tonga-Hunga Ha'apai eruption on 15 January 2022. J. Geophys. Res. Atmos., 128, e2022JD038238. doi:10.1029/2022JD038238.

Bozóki, T., Sátori, G., Williams, E., Guha, A., Liu, Y., et al. 2023. Day-to-day quantification of changes in global lightning activity based on Schumann resonances. J. Geophys. Res. Atmos., 128, e2023JD038557. doi:10.1029/2023JD038557.

Chaffin, J.M., Pu, Y., Smith, D.M., Cummer, S., Splitt, M. 2023. Determining a lower limit of luminosity for the first satellite observation of a reverse beam terrestrial Gamma Ray flash associated with a cloud to ground lightning

leader. J. Geophys. Res. Atmos., 128. doi:10.1029/2023JD038885.

da Silva, C.L., Winn, W.P., Taylor, M.C., Aulich, G.D., Hunyady, S.J., et al. 2023. Polarity asymmetries in rocket-triggered lightning. Geophys. Res. Lett., 50. doi:10.1029/2023GL105041.

Ding, J., Zhang, Y., Zheng, D., Yao, W., Zhang, W. 2023. Thunderstorm and lightning activities over Western Pacific, Northern Indian Ocean and South China Sea along with their adjacent lands. Journal of Tropical Meteorology, 29(3), 347-358.

Ding, Z., Rakov, V.A., Zhu, Y., Kereszy, I., Chen, S., et al. 2023. Propagation mechanism of branched downward positive leader resulting in a negative cloud-to-ground flash. J. Geophys. Res. Atmos., doi:10.1029/2023JD039262.

Efraim, A., Rosenfeld, D., Holzworth, R., Thornton, J.A. 2023. A possible cause for preference of super bolt lightning over the Mediterranean Sea and the Altiplano. J. Geophys. Res. Atmos., 128. doi:10.1029/2022JD038254.

Fan, L., Zhou, C. 2023. Cloud-to-ground and intra-cloud nowcasting lightning using a semantic segmentation deep learning network. Remote Sens., 15. doi:10.3390/rs15204981.

Fan, Y., Zhang, Y., Lyu, W., Ma, Y., Wu, B., et al. 2023. Correlation between frequency-divided magnetic field and channel-base current for rocket-triggered lightning. Remote Sens., 15, 3902. doi:10.3390/rs15153902.

Ghosh, R., Pawar, S.D., Hazra, A., Wilkinson, J., Mudiar, D., et al. 2023. Seasonal and regional distribution of lightning fraction over Indian subcontinent. Earth Space Sci., 10. doi:10.1029/2022EA002728.

Guo, X., Ji, Z., Gao, Y., Zhang, L., Lyu, W., et al. 2023. Effects of positive corona on upward leader initiation from tall building by 3D numerical simulation. Atmos Res, 291, 106822. doi:10.1016/j.atmosres.2023.106822.

Han, B., Tang, J., Zhao, G.Z., Wang, L.F., Dong, Z.Y., et al. 2023. Seasonal and interannual variations in the schumann resonance observed in the ELF electromagnetic networks in China. J. Geophys. Res. Atmos., 128. doi:10.1029/2023JD038602.

Honda, T., Sato, Y., Miyoshi, T. 2023. Regression-based ensemble perturbations for the zero-gradient issue posed in lightning-flash data assimilation with an ensemble Kalman filter. Mon. Wea. Rev., 151, 2573-2586.

Husbjerg, L., Neubert, T., Chanrion, O., Marisaldi, M., Stendel, M., et al. 2023. Characterization of thunderstorm cells producing observable terrestrial Gamma-Ray flashes. J. Geophys. Res. Atmos., 128. doi:10.1029/2023JD038893.

Jensen, D.P., Shao, X., Sonnenfeld, R.G. 2023. Insights into lightning K-Leader initiation and development from three dimensional broadband interferometric observations. J. Geophys. Res. Atmos., 128. doi:10.1029/2023JD039104.

Kalashnikov, D.A., Abatzoglou, J.T., Loikith, P.C., Nauslar, N.J., Bekris, Y., et al. 2023. Lightning-ignited wildfires in the western United States: Ignition precipitation and associated environmental conditions. Geophys. Res. Lett., 50. doi:10.1029/2023GL103785.

Koike, S., Fukuyama, M., Baba, Y., Tsuboi, T., Rakov, V.A. 2023. Reconstruction of lightning return-stroke current waveforms from electromagnetic field waveforms degraded by propagation effects. IEEE Transactions on EMC, doi:10.1109/TEMC.2023.3325280.

Kutsuna, K., Nagaoka, N., Baba, Y., Tsuboi, T., Rakov, V.A. 2023. Estimation of lightning channel-base current from far electromagnetic field in the case of inclined channel. Electr. Pow. Syst. Res., 214, 108854. doi:10.1016/j.epsr.2022.108854.

Lang, T.J. 2023. Validation of the geostationary lightning mapper with a lightning mapping array in Argentina: Implications for current and future spaceborne lightning observations. Earth Space Sci., 10. doi:10.1029/2023EA002998.

Liu, D., Yu, H., Sun, C. 2023. Estimation of lightning activity of squall lines by different lightning parameterization schemes in the weather research and forecasting model. Remote Sens., 15. doi:10.3390/rs15205070.

Malecic, B., Cui, R., Demory, M.E., Horvath, K., Jelic, D., et al. 2023. Simulating hail and lightning over the Alpine Adriatic region: A model intercomparison study. J. Geophys. Res. Atmos., 128. doi:10.1029/2022JD037989.

Mondal, U., Sreelekshmi, S., Panda, S.K., Kumar, A., Das, S., et al. 2023. Diurnal variations in lightning over India and three lightning hotspots: A climatological study. J. Atmos. Sol.-Terr. Phy., 252. doi:10.1016/j.jastp.2023.106149.

Morvais, F., Liu, C. 2023. Estimation of lightning flash rate in precipitation features by applying shallow AI neural network models to the GMI passive microwave brightness temperatures. J. Geophys. Res. Atmos., 128. doi:10.1029/2023JD039516.

Nag, A., Cummins, K.L., Plaisir, M.N., Brown, R.G., Wilson, J.G., et al. 2023. Characteristics of upward-connecting-leader current leading to attachment in downward negative cloud-to-ground lightning strokes. Atmos. Res., 294. doi:10.1016/j.atmosres.2023.106943.

Nag, A., Khounate, H., Cummins, K.L., Goldberg, D.J., Imam, A.Y., et al. 2023. Parameters of the lightning attachment processes in a negative cloud-to-ground stroke observed on a microsecond timescale. Geophys. Res. Lett., 50. doi:10.1029/2023GL104196.

Neto, O.P., Pinto, I.R.C.A., Pinto Junior, O., Williams, E.R. 2023. Evidence of a link between Amazon fires and lightning. J. Atmos. Sol.-Terr. Phy., 249. doi:10.1016/j.jastp.2023.106095.

Ni, X., Huang, F., Hui, W., Xiao, H. 2023. Lightning evolution in hailstorms from the geostationary lightning mapper over the Contiguous United States. J. Geophys. Res. Atmos., 128. doi:10.1029/2023JD038578.

Pailoor, N., Cohen, M., Richardson, D., Harid, V., Golkowski, M. 2023. Quantification of lightning-induced electron precipitation events on electron fluxes in the radiation belts. J. Geophys. Res. Space Physics., 128. doi:10.1029/2022JA031153.

Pan, Y., Zheng, D., Zhang, Y., Lu, G., Yao, W., et al. 2023. An investigation on spatiotemporal sizes of specific types of lightning flashes. J. Geophys. Res. Atmos., 128, e2022JD038191. doi:10.1029/2022JD038191.

Perez-Invernon, F.J., Moris, J.V., Gordillo-Vazquez, F.J., Fullekrug, M., Pezzatti, G., et al. 2023. On the role of continuing currents in lightning-induced fire ignition. J. Geophys. Res. Atmos., 128. doi:10.1029/2023JD038891.

Peterson, M. 2023. A survey of thunderstorms that produce megaflashes across the Americas. Earth Space Sci., 10. doi:10.1029/2023EA002920.

Peterson, M. 2023. Interactions between lightning and ship traffic. Earth Space Sci., 10. doi:10.1029/2023EA002926.

Peterson, M. 2023. Making a superbolt: Reconciling observations of the optically brightest lightning on Earth from different satellites. Earth Space Sci., 10. doi:10.1029/2023EA003001.

Peterson, M. 2023. WWLLN energetic lightning events are different from optical superbolts. Geophys. Res. Lett., 50. doi:10.1029/2023GL104074.

Qi, Q., Wu, B., Lyu, W., Ma, Y., Chen, L., et al. 2023. The attachment process of negative connecting leader to the lateral surface of downward positive leader in a positive cloud-to-ground lightning flash. Geophys. Res. Lett., 50. doi:10.1029/2023GL104887.

Saha, J., Price, C., Guha, A. 2023. Are thunderstorms linked to the rapid sea ice loss in the Arctic? Atmos. Res., 294. doi:10.1016/j.atmosres.2023.106988.

Saha, J., Price, C., Guha, A. 2023. The role of global thunderstorm activity in modulating global cirrus clouds. Geophys. Res. Lett., 50, e2022GL102667. doi:10.1029/2022GL102667.

Saleh, N., Gharaylou, M., Farahani, M.M., Alizadeh, O. 2023. Performance of lightning potential index, lightning threat index, and the product of CAPE and precipitation in the WRF model. Earth Space Sci., 10. doi:10.1029/2023EA003104.

Schenkel, B.A.A., Calhoun, K.M.M., Sandmael, T.N.N., Fruits, Z.R.R., Schick, I., et al. 2023. Lightning and radar characteristics of tornadic cells in landfalling tropical cyclones. J. Geophys. Res. Atmos., 128. doi:10.1029/2023JD038685.

Slocum, C.J., Knaff, J.A., Stevenson, S.N. 2023. OPERATIONAL PREDICTION SYSTEM NOTES (OPS NOTES) lightning-based tropical cyclone rapid intensification guidance. Weather Forecast., 38, 1209-1227.

Stock, M., Tilles, J., Taylor, G.B., Dowell, J., Liu, N. 2023. Lightning interferometry with the long wavelength array. Remote Sens., 15. doi:10.3390/rs15143657.

Syssoev, A.A., Iudin, D.I. 2023. Numerical simulation of electric field distribution inside streamer zones of positive and negative lightning leaders. Atmos. Res., 295. doi:10.1016/j.atmosres.2023.107021.

Tang, G., Jiang, R., Sun, Z., Liu, M., Zhang, H., et al. 2023. Characteristics of negative breakdowns in extinguished channels of a positive cloud-to-ground flash. Atmos. Res., p.106895.

Thiel, K.C., Calhoun, K.M., Reinhart, A.E. 2023. Forecast applications of GLM gridded products: A data fusion perspective. Weather Forecast., 38, 2253-2270.

Tinsley, B.A. 2023. Solar activity, weather and climate: The elusive connection. Bull. Am Meteorol. Soc., doi:10.1175/BAMS-D-23-0065.1.

Tsurumi, M., Enoto, T., Ikkatai, Y., Wu, T., Wang, D., et al. 2023. Citizen science observation of a Gamma-Ray glow associated with the initiation of a lightning flash. Geophys. Res. Lett., 50. doi:10.1029/2023GL103612.

Van Eaton, A.R., Lapierre, J., Behnke, S.A., Vagasky, C., Schultz, C.J., et al. 2023. Lightning rings and gravity waves: Insights into the giant eruption plume from Tonga's Hunga volcano on 15 January 2022. Geophys. Res. Lett., 50. doi:10.1029/2022GL102341.

Wang, F., Zhang, Y., Chen, L., Zhang, Y., Yao, W., et al. 2023. Climatology of large peak current cloud-to-ground lightning flashes in China's most populous areas. Earth Space Sci., 10, e2023EA003202. doi:10.1029/2023EA003202.

Wemhoner, J., Wermer, L., da Silva, Caitano L. da, Barnett, P., et al. 2023. Lightning radiometry in visible and infrared bands. Atmos. Res., 292. doi:10.1016/j.atmosres.2023.106855.

Wu, B., Qi, Q., Lyu, W., Ma, Y., Chen, L., et al. 2023. High-speed video observations of needles evolving into negative leaders in a positive cloud-to-ground lightning flash. J. Geophys. Res. Atmos., 128, e2023JD039523. doi:10.1029/2023JD039523.

Wu, T., Wang, D., Takagi, N. 2023. High-accuracy classification of radiation waveforms of lightning return strokes. J. Geophys. Res. Atmos., 128. doi:10.1029/2023JD038715.

Xiang, T., Liu, M., He, S., Zhou, C. 2023. Assimilation and inversion of ionospheric electron density data using lightning whistlers. Remote Sens., 15. doi:10.3390/rs15123037.

Xiao, L., Chen, W., Wang, Y., Bian, K., Fu, Z., et al. 2023. Toward an interpretable CNN

model for the classification of lightning-produced VLF/LF signals. J. Geophys. Res. Atmos., 128. doi:10.1029/2023JD039517.

Xu, C., Huret, N., Celestin, S., Qie, X. 2023. Detailed modeling and evaluation of the potential impact of blue jet on the atmospheric chemistry. J. Geophys. Res. Atmos., 128, e2023JD038668. doi:10.1029/2023JD038668.

Yair, Y., Korman, M., Price, C., Stybbe, E. 2023. Observing lightning and transient luminous events from the international space station during ILAN-ES: An astronaut's perspective. Acta Astronautica, 211, 592-599.

Yair, Y., Yaniv, R. 2023. The effects of fog on the atmospheric electrical field close to the surface. Atmosphere, 14, 549. doi:10.3390/atmos14030549.

Yaniv, R., Yair, Y., Price, C., Reuveni, Y. 2023. No response of surface-level atmospheric electrical parameters in Israel to severe space weather events. Atmosphere, 14, 1649. doi:10.3390/atmos14111649.

Zhang, D., Cummins, K.L., Lang, T.J., Buechler, D., Rudlosky, S. 2023. Performance evaluation of the lightning imaging sensor on the international space station. J. Atmos. Oceanic Technol., 40, 1063-1082.

Zhang, H., Zhang, Y., Fan, Y., Zhang, Y., Krehbiel, P.R., et al. 2023. Guangdong lightning mapping array: Errors evaluation and preliminary results. Earth Space Sci., 10. doi:10.1029/2023EA003143.

Zhang, Y., Cao, D., Yang, J., Lu, F., Wang, D., et al. 2023. A parallax shift effect correction based on cloud top height for FY-4A Lightning Mapping Imager (LMI). Remote Sens., 15. doi:10.3390/rs15194856.

Zheng, D., Fan, P., Zhang, Y., Yao, W., Fang, X., et al. 2023. Deep convective clouds observed by ground-based radar over Naqu, Qinghai-Tibet Plateau. Atmos Res, 293, 106930. doi:10.1016/j.atmosres.2023.106930.

Zou, M., Zhang, Y., Tan, Y., Chen, L., Yao, W. 2023. Observation and simulation of lightning strikes in an offshore wind turbine cluster. Earth Space Sci., 10, e2022EA002809. doi:10.1029/2022EA002809.

ATMOSPHERIC ELECTRICITY

NEWSLETTER

Vol.34 No.2 2023 Nov

Edited by: Wenjuan Zhang (CAMS) and Haiyang Gao (NUIST)

REMINDER

Newsletter on Atmospheric Electricity presents twice a year (May and November) to the members of our community with the following information:

- ✧ announcements concerning people from atmospheric electricity community, especially awards, new books...,
- ✧ announcements about conferences, meetings, symposia, workshops in our field of interest,
- ✧ brief synthetic reports about the research activities conducted by the various organizations working in atmospheric electricity throughout the world, and presented by the groups where this research is performed, and
- ✧ a list of recent publications. In this last item will be listed the references of the papers published in our field of interest during the past six months by the research groups, or to be published very soon, that wish to release this information, but we do not include the contributions in the proceedings of the Conferences.

No publication of scientific paper is done in this Newsletter. We urge all the groups interested to submit a short text (one page maximum with photos eventually) on their research, their results or their projects, along with a list of references of their papers published during the past six months. This list will appear in the last item. Any information about meetings, conferences or others which we would not be aware of will be welcome.

Call for contributions to the newsletter

All issues of this newsletter are open for general contributions. If you would like to contribute any science highlight or workshop report, please contact Weitao Lyu (weitao.lyu@gmail.com) preferably by e-mail as an attached word document.

The deadline for **2024 spring issue** of the newsletter is **May 15, 2024**.

PRESIDENT
Xiushu Qie
Chinese Academy of Sciences
E-mail: qiex@mail.iap.ac.cn

SECRETARY
Weitao Lyu
Chinese Academy of Meteorological Sciences
E-mail: weitao.lyu@gmail.com

ICAE

IAMAS IUGG